5-16-2022

Microbial Experience Increases Cytotoxicity of Tumor-Infiltrating CD8+ T Cells and Controls Tumor Growth

Nicholas Aaron Bunda
Grand Valley State University

ScholarWorks Citation

Microbial Experience Increases Cytotoxicity of Tumor-Infiltrating CD8+ T Cells and Controls
Tumor Growth

Nicholas Aaron Bunda

A Thesis Submitted to The Graduate Faculty of

GRAND VALLEY STATE UNIVERSITY

In

Partial Fulfillment of the Requirements

For the Degree of

Master of Health Sciences

Biomedical Sciences

April 2022

THESIS APPROVAL FORM

GRANDVALLEY
STATE UNIVERSITY

The signatories of the committee members below indicate that they have read and approved the thesis of Nicholas Aaron Bunda in partial fulfillment of the requirements for the degree of Master of Health Science in Biomedical Sciences.

Dr. Kristin Renkema, Thesis committee chair   4/4/22   Date

Dr. Christopher Pearl, Committee member   4-4-22   Date

Dr. Frank Sylvester, Committee member   4-4-22   Date

Accepted and approved on behalf of the
College of Liberal Arts and Sciences

Dean of the College
5/16/2022

Date

Accepted and approved on behalf of the
Graduate Faculty

Associate Vice-Provost for the Graduate School

5/16/2022

Date

ACKNOWLEDGEMENTS

This thesis was truly a team effort, and I owe a debt of gratitude to many people. First and foremost, I want to thank and acknowledge my mentor, Dr. Kristin Renkema. She is truly fearless, a quality of hers that I admire most. She continually championed my ambitious and lofty research goals without hesitation, even when they made her life more difficult. This is a testament to her passion for the field of immunology, and a prime example of her collaborative brand of leadership. Thanks to her, I presented these findings at the Autumn Immunology Conference, published an abstract at the Midwinter Conference of Immunologists, and was selected for GVSU's Graduate Student Showcase. I also received the Excellence-in-a-Discipline Award from the department of Biomedical Sciences, an accomplishment that would not have been possible without Kristin. I am so grateful for her mentorship and her friendship. I will undoubtedly be a better physician and scientist for having known her.

I also want to thank my fellow graduate student, Marlee Busalacchi. Thank you for agreeing to start harvest days at 7:00 AM, for labelling thousands of tubes, for being a problem solver, for stress-eating carrot cake in the hallway with me, and for always letting me pick the music. Thank you for your friendship, Frances!

I'd like to thank Dr. Chris Pearl and Dr. Frank Sylvester for serving on my committee, Roland Nulph and Maci Rozich for their help with the mice, and the Graduate School for supporting this work with a Presidential Research Grant. Special thanks to the grad room crew, Caleb and Ali Camero, for your friendship and encouragement.

Finally, I would like to thank my wife, Jeannette, and my three kids, Jackson, Sloane, and Beau. Nobody has sacrificed more for this thesis than you kids. I hope it will serve as a reminder to pursue your passions and stay curious about the world around you.

ABSTRACT

Cancer immunotherapy research is traditionally conducted with specific pathogen-free (SPF) mice, which most accurately mimic the immune system of a human newborn. This makes translational research challenging, as this mouse model is not an accurate reflection of the adult patients who ultimately receive newly developed treatments. It is necessary to further develop a mouse model that bridges this gap and increases translatability of current cancer immunotherapy research.

By cohousing specific pathogen-free mice with regular pet store (PS) mice, we have generated a cohoused (CoH) mouse that reflects the microbial experience of an adult human immune system. We investigated antigen experience, differentiation, and cytotoxicity of CD8+ T cell populations within the tumor microenvironment of both SPF and CoH mice by injecting them with B16-melanoma. We also investigated the impact of microbial experience on PD-1 expression. Increased PD-1 expression indicates a state of T cell exhaustion and may act to modulate the efficacy of anti-PD-1/anti-CTLA-4 immunotherapies. This efficacy was tested with a novel *in vitro* checkpoint blockade assay.

Here, we show that CoH mice exhibit significantly increased populations of antigen experienced, differentiated, and cytotoxic CD8+ T cells in blood, spleen, tumor-draining lymph nodes, and tumor. CD8+ T cells of CoH mice also exhibit significantly increased PD-1 expression and slight increases in the efficacy of *in vitro* anti-PD-1 immunotherapy. Most importantly, our data show that CoH mice have superior anti-tumor immunity as evidenced by their significantly lower tumor weights when compared to the larger tumors of SPF mice. Taken together, our results show that microbial experience increases cytotoxicity of tumor-infiltrating CD8+ T cells and controls tumor growth.

4

TABLE OF CONTENTS

LIST OF TABLES

LIST OF FIGURES

9

ABBREVIATIONS

SPF: specific pathogen-free mice; C57BL/6 strain with no microbial exposure

CoH: cohoused mice; SPF mice cohoused in the same cage with PS mouse for 28 days

PS: pet store mice; commercially purchased mice with various microbial exposures

KLRG1: killer cell lectin-like receptor G1; marker of antigen-experience and differentiation

GzB: Granzyme B; effector molecule of CD8+ T cells

PD-1: programmed death receptor 1; marker of T cell exhaustion

PD-L1: programmed death ligand 1; binds PD-1 to downregulate T cell effector function

CTLA-4: cytotoxic T-lymphocyte-associated protein 4; downregulates T cell effector function when bound

dLN: draining lymph node samples

LLECs: long-lived effector cells

IFN-γ: Interferon γ (gamma); cytokine released by CD8+ T cells upon activation

ELISA: enzyme-linked immunosorbent assay; used to measure concentrations of IFN-γ in serum and supernatant samples

CHAPTER 1: INTRODUCTION

The immune system provides the first line of defense against cancer development. This defense system is comprised of a rapidly responding, non-specific, innate immune system, as well as a highly-specific adaptive immune system. The cells of the adaptive immune system, CD8+ T cells in particular, regularly detect and kill cancerous cells. Various populations of these CD8+ T cells develop throughout the process of aging, largely as a result of continuous exposures to disease-causing organisms (called pathogens) and cancerous cells.

Traditional cancer immunology research is conducted with standard laboratory mice that are raised under specific-pathogen-free conditions, and most accurately mimic the immune system of a human newborn (Beura et al., 2016). In stark contrast with adults, newborns possess no immune memory, resulting in a slower immune response to microbial invaders. While the use of SPF mice provides researchers with a highly reliable and genetically predictable animal model, it offers a poor analogue of the diversely sensitized adult human immune system (Masopust et al., 2017). Therefore, cancer immunotherapy research conducted solely in SPF mice fails to account for a variety of modulating interactions that may occur within a microbially experienced host.

There is a need to further develop a cohoused (CoH) mouse model that more accurately recapitulates the human tumor microenvironment. It has already been established that cohousing SPF mice with pet store mice (PS) leads to the development of more antigen-experienced immune cells (Beura et al., 2016), and using this model could provide a better understanding of how prior infection and microbial exposures impact immune responses to cancer. Furthermore, if microbial experience shapes the development and differentiation of the T cell repertoire, then microbial experience may also impact the efficacy of many commonly used immunotherapies.

The advent of checkpoint blockade immunotherapies marked the most significant cancer treatment advancement since the early 1900's. Researchers discovered a receptor that cancer cells use to "shut off" the immune response of CD8+ T cells (Leach, Krummel, & Allison, 1996). Programmed cell Death-1 (PD-1) and Cytotoxic-T-Lymphocyte Associated protein 4 (CTLA-4) are receptors that are expressed on the surface of CD8+ T cells. Both receptors are capable of interacting with ligands expressed on the surface of tumor cells. Through this interaction, tumor cells are able to inhibit CD8+ T cell anti-tumor effector functions, allowing cancerous cells to survive and continue replicating. Through administration of antibodies designed to bind these receptors (anti-PD-1 & anti-CTLA-4), tumor cells aren't able to interact with PD-1 and CTLA-4, thus eliminating the tumor cells ability to inhibit and evade the anti-tumor immune response. These treatments effectively preserve CD8+ T cell killing of cancerous cells (Leach, Krummel, & Allison, 1996; Phan et al., 2003; Blank et al., 2004; Miller & Carson, 2020).

In a clinical study of advanced metastatic melanoma, a 5-year overall survival rate of 34% was observed in patients taking an anti-PD-1 immunotherapy called pembrolizumab (Hamid et. al, 2019). While these treatments have saved thousands of lives, the nuance of their mechanisms remain incompletely characterized, as evidenced by large patient populations that remain unresponsive to immune checkpoint therapies (Padmanee & Allison, 2015). Challenges regarding efficacy may be due to the variability of the tumor microenvironment from one patient to the next. We believe this heterogeneity may be due, in part, to individual variation in microbial exposure and its long-term impact on proliferation and differentiation of effector CD8+ T cell populations.

Differences in PD-1 and CTLA-4 expression may exist between SPF and CoH mice, and this may result in CD8+ T cell populations with differing anti-tumor properties. Through treatment with anti-PD-1 and/or anti-CTLA-4, cytotoxicity may be rescued, allowing for characterization of the differences in anti-tumor effector function that exist between SPF and CoH mice.

Purpose

Previous research conducted in the Renkema lab showed that robust microbial experience may impact the proliferation of antigen experienced tumor-infiltrating CD8+ T cells in response to B16 melanoma. However, variation in effector function remains largely uncharacterized (Groeber, 2020). Here, we further examine this variation in effector function between SPF and CoH mice, while also exploring difference in cytotoxicity within the context of checkpoint blockade immunotherapy. Additionally, we investigate how microbial experience impacts growth and size of the tumor.

Scope

This work is focused on variation in tumor-infiltrating CD8+ T cell proliferation, activation, differentiation, cytotoxicity, and exhaustion/anergy in SPF versus CoH mice. These differences are analyzed by flow cytometry of *ex vivo* tissue samples, as well as *in vitro* T cell stimulation cultures. *In vitro* checkpoint blockade assays utilize anti-PD-1 and/or anti-CTLA-4 antibodies as treatment conditions in T cell cultures. Variation in cytotoxicity in response to treatment is measured by concentrations of Granzyme B.

Assumptions

Previous cohorts of mice were successfully cohoused (Groeber, 2020), so it is assumed that future cohorts of SPF and PS mice will be cohoused successfully by following the labs existing protocols. Additionally, previous cohorts of mice were injected with cultured B16 melanoma cells and tumor growth was observed in 5-14 days. It is assumed that this can be replicated in future cohorts. Finally, the immune response is assumed to be different between SPF and CoH mice.

Hypothesis

We hypothesize that microbial experience increases CD8+ T cell-mediated anti-tumor immunity and controls tumor growth.

Significance

Humans are continuously exposed to pathogens from the environment and cancerous cells within the body. These exposures shape the development and differentiation of T cell populations. The adaptive immune system of an adult human is dynamic and ever-changing, and modern research models should strive to recreate the same dynamism. The cohoused mouse model has the potential to improve translational research in cancer immunotherapy by providing a complementary mouse model that more accurately mimics the adult human immune system. Furthermore, cohoused mice can help provide an understanding of how microbial experience impacts immune responses to cancer and variations in immunotherapeutic efficacy.

CHAPTER 2: LITERATURE REVIEW

The Immune System

The immune system provides the first line of defense against cancer development. This defense system is comprised of a rapidly responding, non-specific, innate immune system, as well as a highly-specific adaptive immune system. The innate immune system includes physical barriers like the skin and mucous membranes, the acidic pH of stomach acid, non-specific phagocytes like dendritic cells and macrophage that kill and digest whole organisms, and antibacterial serum proteins that mediate inflammation. In addition to these pathogen-mediated immune mechanisms, the innate immune system also stimulates the adaptive immune response to pathogens and cancerous cells through inflammation. The innate immune system also activates the adaptive immune response, primarily by presenting digested pieces (antigen) of disease-causing organisms (pathogens) or cancerous cells to adaptive immune cells. This function is mediated by antigen-presenting cells (APC's), like dendritic cells and macrophages, which present antigen on a group of surface glycoproteins called major histocompatibility complex (MHC). APC's will present digested "non-self" antigen from exogenous or extracellular pathogens (like bacteria) on class II MHC molecules. Additionally, class I MHC molecules exist on all nucleated cells and present endogenous or intracellular "self" antigen, including cancer antigen (Marshall et al., 2018).

The cells of the adaptive immune system include antigen-specific T cells and B cells. Both cell types are able to distinguish between "self" and "non-self" antigen through the use of highly specific T cell receptors (TCR) and B cell receptors (BCR). BCRs are immunoglobulin G antibodies with heavy and light chain variable regions that undergo random recombination to produce 10^6 unique BCRs. Similarly, TCRs are composed of an extracellular α and β chain, each

with a variable and hypervariable region also capable of producing approximately 10^6 unique TCRs. TCR and BCR recombination allows for the generation of highly diverse and highly specific antigen receptors. A mechanism of central tolerance called negative selection occurs during T and B cell development, effectively eliminating T and B cells that possess "self" antigen reactive TCRs and BCRs. As such, B and T cells should not be activated by healthy cells presenting "self" antigen on class I MHC (Marshall et al., 2018). In the context of cancer, activation of CD8+ T cells through TCR stimulation by antigen-presenting MHC-I is inhibited by receptors expressed on cancerous cells via mechanisms discussed in a future section.

T cells circulate throughout the body via the lymphatic system and blood stream. When APC's present antigen, TCR-MHC interactions induce proliferation of subsets of T-helper (Th) cells (CD4+ T cells) and cytotoxic T cells (CD8+ T cells). CD4+ T cells cannot directly kill infected cells or phagocytize pathogens, but they regulate the adaptive immune response through secretion of various cytokines, and are also responsible for B cell activation via class II MHC-TCR interaction. Upon stimulation by Th cells, B cells differentiate into memory B cells and antibody-producing plasma cells that provide humoral immunity (Marshall et al., 2018).

Unlike Th cells, CD8+ T cells directly kill infected and cancerous cells. CD8+ T cells require three signals for activation to occur. First, the TCR of a naïve CD8+ T cell will interact with class I MHC molecules on an APC. The second signal is co-stimulation between CD28 on the T cell and CD80/86 on the APC. These first two steps are enough to stimulate proliferation of this antigen-specific CD8+ T cell population. In the third and final signal, stimulation by interleukin-2 (IL-2) is required for survival, and stimulation by interleukin-12 (IL-12) and type I interferons are required to confer full effector function (Mescher et al., 2006; Curtsinger et al., 2007). "Effector function" refers to the CD8+ T cells ability to kill infected or cancerous cells.

Exposure to signal 3 cytokines upregulates expression of perforin and granzyme B within the CD8+ T cell. Perforin is a protein that forms pores in the target cell, allowing granzyme B, a serine protease, to enter the target cell and induce apoptosis by activating the caspase cascade (Andersen et al., 2006; Mescher et al., 2006; Curtsinger et al., 2007).

A distinguishing characteristic of the adaptive immune response is memory. After the initial immune response has cleared the infected or cancerous cells, most of the activated CD8+ T cells will die. However, a small percentage of the cells will downregulate their effector function, while still retaining the ability to rapidly reactivate and expand upon restimulation by the same pathogen. However, effector memory CD8+ T cells have been shown to circulate in the blood and position themselves to intercept invading pathogens. This effector memory pool of CD8+ T cells retains high expression of cytolytic activity after contraction of the primary immune response. When activated by the same pathogen a second time, these populations of effector memory CD8+ T cells expand earlier in the course of infection due to increased starting pools compared to naïve T cells of the primary immune response. The secondary immune response is also faster because memory T cells have a lower threshold of activation, requiring lower amounts of antigen and co-stimulation. Additionally, activated effector memory CD8+ T cells exhibit increased cytokine production and a more rapid upregulation of Granzyme B compared to naïve T cells. Taken together, the secondary immune response of CD8+ T cells is more rapid and cytotoxic (Masopust & Schenkel, 2013; DiSpirito & Shen, 2010).

Continual exposure to environmental pathogens and cancerous cells results in the development of diverse populations of memory T cells and changes in overall immune function. In one study, researchers found that persistent viral infection with murine cytomegalovirus irreversibly diminished the presence of naïve CD8+ T cells (Cicin-Sain et al., 2012). If a

persistent viral infection has the ability to irreversibly reduce specific populations of T cells, then great variation in the memory CD8+ T cell repertoire must exist from person to person, as humans are frequently exposed to a wide variety of viruses and infectious pathogens. The type and frequency of microbial exposure may vary significantly from person to person. Since memory CD8+ T cell populations are shaped by these environmental stimuli, it may result in highly individualized immune systems. This heterogeneity has led to translational challenges within immunotherapeutic research.

Limitations of Specific-Pathogen-Free Mice in Immunology Research

Specific pathogen-free mice have long been used in cancer and biomedical research. Mendelian heritability was first studied in mammals around 1902, and quickly led to the development of inbreeding the common house mouse (*Mus musculus domesticus*) as a means of controlling genetic expression. These methods gave rise to the C57BL/6 strain, now one of the most widely used strains of laboratory mice (Morse III, 2007; Sellers et al., 2012). In addition to the genetic stability of these mice, they are also raised and housed under "SPF conditions," which include a plethora of biocontainment procedures and safeguards. They are kept in microisolation cages with filtered tops to prevent the introduction of pathogens, and aseptic technique is used when handling. Additionally, all food and equipment coming in contact with the mice is sterilized (Masopust et al., 2017).

Unlike SPF mice, wild mice must compete for food and resources. They are also continually exposed to environmental antigens, which means the immune response of wild mice contributes greatly to their fitness for survival (Abolins et al., 2017). Much like humans, wild mice live in genetically diverse populations, and freedom of movement allows for constant

microbial exposure. As such, understanding the differences in immune function and development amongst SPF and wild mice will be critical for any research with translational goals.

While the use of SPF mice provides researchers with a highly reliable and genetically predictable animal model, it also provides major variability in resistance and susceptibility to infectious disease within many inbred strains. For example, C57BL/6 mice have a unique resistance to murine cytomegalovirus due to expression of the *Klra8* gene. Additionally, C57BL/6 mice have been shown to have a Th1 bias, while other commonly used mouse strains exhibit a Th2 bias. Segregation into Th1 and Th2 helper T cell populations is dependent on cytokines released by APCs during an immune response. Th1 populations are important for clearance of intracellular pathogens like viruses and cancers, while Th2 populations are important for parasitic infections. These examples of immune dysfunction have been mapped to specific loss of function mutations in genes that affect the immune response, and should be considered before selecting a mouse model (Sellers et al., 2012). Taken together, SPF mice offer a poor analogue of the diversely sensitized adult human immune system, while also introducing additional mutations that may confound results.

Cohoused Mice Recapitulate the Immune System of an Adult Human

Researchers at the University of Minnesota developed a novel cohousing model to investigate the affect of environmental conditions on the differentiation and distribution of CD8+ T cells within genetically stable C57BL/6 mice (Beura et al., 2016). Commercially purchased pet store mice were introduced into cages of SPF mice (C57BL/6 strain) for a period of four weeks (Figure 1). Through cohousing, SPF mice were exposed to various murine pathogens carried by

the pet store mice. Weekly blood samples were taken to monitor immune cell changes within

SPF mice.
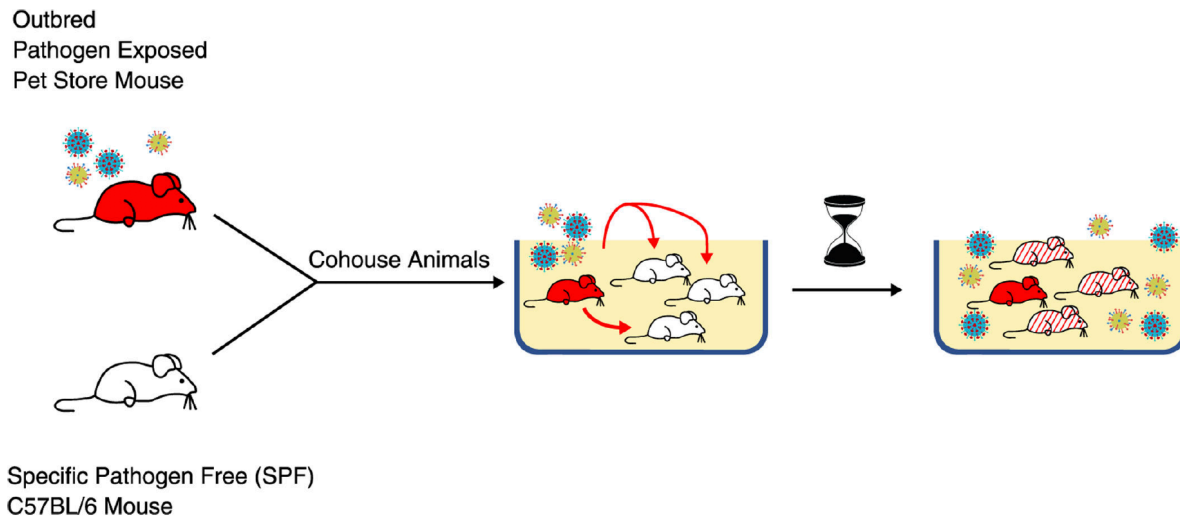
Figure 1: Methods of Cohousing Mice.
Cohousing pet store with SPF mice induces a shift from naïve (CD44^{lo}) to antigen-experienced (CD44^{hi}) CD8+ T cells in SPF mice (Huggins et al., 2019).

Before cohousing, the Beura study revealed that antigen-experienced/memory CD8+ T

cells were almost entirely absent in SPF mice, but were observed in feral barn mice and

commercially purchased pet store mice. This difference suggests that the environment plays a

role in shaping the development of these CD8+ T cell populations. Additionally, CD8+ T cells

with a CD27^{lo}Granzyme B+ phenotype are considered cytotoxic and capable of responding to

infection. Of the few antigen-experienced/memory CD8+ T cells observed in SPF mice, almost

none expressed this cytotoxic phenotype.

After the cohousing period, CoH mice exhibited increased antigen-experienced CD8+ T

cell populations with CD44^{hi} phenotype, while the SPF mice (used as negative controls)

remained naïve or antigen-inexperienced with a CD44^{lo} phenotype. CD44 is a T cell surface

marker that is upregulated and maintained on both effector and memory T cells in response to

TCR engagement or cytokine signaling (Baaten et al., 2010). CD44^{hi} CD8+ T cells increased

from 15% to 70% in cohoused mice. Additionally, SPF mice lacked effector-differentiated

memory T cells that were present in feral and pet store mice (Figure 2), as indicated by decreased

expression of KLRG1 and Granzyme B. KLRG1 is an indicator of terminal differentiation or

senescence, and is found to be upregulated on long-lived effector cells (LLECs). Taken together,

these results indicate that antigen-experienced CD44^{hi} CD8+ T cell populations can be induced

in genetically stable SPF mice through environmental exposure (Beura et al., 2016).
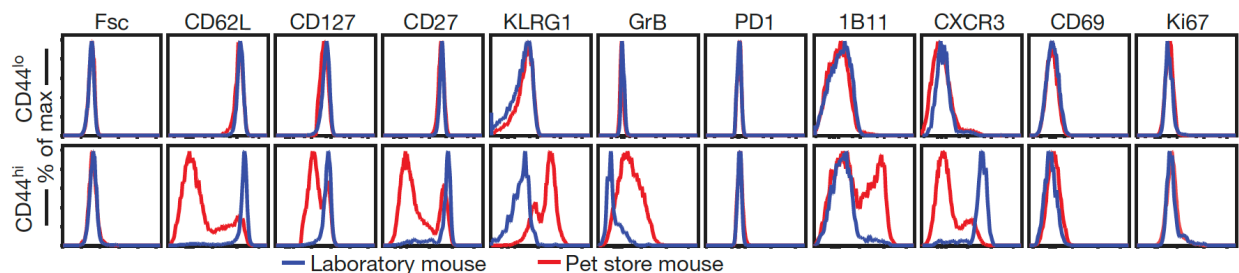
Figure 2: Differentiation markers of antigen-experienced (CD44^{hi}) and naïve (CD44^{lo}) CD8+ T cells in laboratory and pet store mice.
Naïve CD8+ T cells in laboratory and pet store mice are phenotypically identical. Antigen-experienced CD8+ T cells from pet store mice show increased expression of Granzyme B and CD27lo cells, as well as increased signals of terminal effector differentiation (Beura et al., 2016).

A metagene analysis revealed that gene expression profiles of cohoused mice more

closely reflected that of an adult human, while SPF mice mimic the immune system of a human

newborn (Beura et al., 2016). In stark contrast with adults, newborns have a restricted TCR

repertoire and possess little immune memory, limiting their protection against microbial

challenge (Rudd, 2020). Therefore, research conducted solely in SPF mice fails to account for a

variety of modulating interactions that may occur within a microbially experienced host.

Cohousing mice allows genetic stability to be maintained, while more accurately recapitulating

the adult human immune system, thus providing a necessary complement to the existing SPF

models (Figure 3).
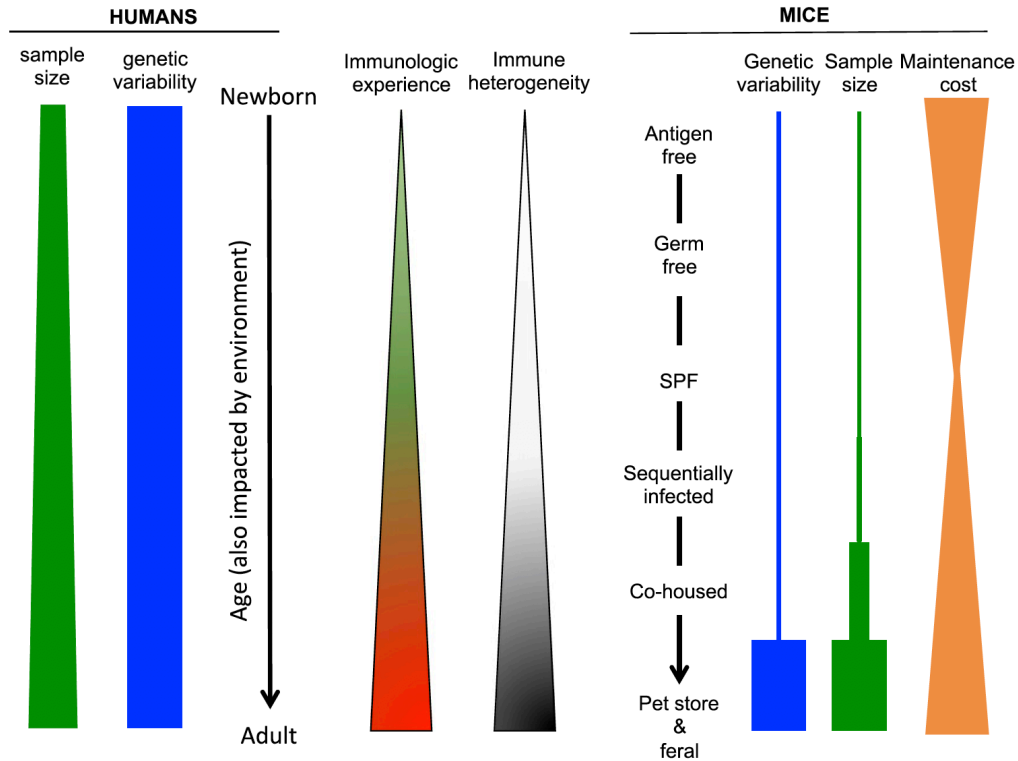
Figure 3: Cohoused mice maintain genetic stability while more accurately mimicking an adult human immune system.
Cohousing C57BL/6 mice (SPF) with commercially purchased pet store mice effectively generates CD8+ T cell populations that otherwise do not exist in SPF mice alone. This model maintains the genetic stability provided by SPF mice, while recapitulating the immune system of an adult human through microbial exposure (Masopust et al., 2017).

Cancer Development & The Tumor Microenvironment

Cancer occurs when healthy cells begin to divide uncontrollably. Cancerous cells are

genetically similar to healthy cells, and they initially continue expression of "self" antigen on

class I MHC molecules. However, during neoplastic transformation, cancerous cells will begin

expressing neoantigens called tumor-associated antigens (TAAs). TAAs are recognized by the

immune system as "non-self" antigen, and will elicit an immune response. The immune system is

capable of lysing a few cancerous cells, but cancerous cells have many hallmark characteristics that allow them to persist. These hallmarks include avoiding immune destruction, enabling replicative immortality, tumor-promoting inflammation, activating invasion & metastasis, inducing or accessing vasculature, genome instability & mutation, resistance to cell death, deregulation of cell metabolism, sustained proliferative signaling, and evasion of growth suppressors (Hanahan, 2022; Hanahan & Weinberg, 2011). These hallmarks are all necessary for tumor growth and progression.

Recent studies have provided insight into how the microbiome impacts tumor progression and immunotherapeutic efficacy. One such study in a model of colon cancer has shown that some bacteria (*Enterococcus sp.* and others) express a peptidoglycan hydrolase called SagA that releases mucopeptides from the bacterial wall. These mucopeptides then circulate systemically and activate the NOD2 pattern receptor, which has been shown to enhance T-cell responses and improve the efficacy of checkpoint blockade immunotherapies (Griffin et. al, 2021). Another study has shown that bacteria can actually be detected within solid tumors in mouse models of lung and pancreatic cancers (Pushalkar et. al, 2018; Jin et. al, 2019). Further investigation of microbial influence on tumor progression is needed in additional cancer types.

Melanoma constitutes approximately 5% of all skin cancers, but is responsible for more than 75% of skin cancer deaths. This is due, in part, to the propensity of melanoma to metastasize to other organ systems, most commonly the brain (Rebecca et al., 2020). Currently, there is no published work investigating B16 melanoma in a model utilizing microbially experienced cohoused mice. However, subcutaneous injection of B16 melanoma in C57BL/6 mice is a well-established and widely used protocol within the field of cancer immunology (Overwijk & Restifo, 2001). Previous researchers in the Renkema lab successfully injected and

grew B16 melanoma tumors in cohoused mice (Groeber, 2020). That work focused on

characterization of tumor-infiltrating CD8+ T cells, but did not investigate the impact of

microbial experience on B16 melanoma cell phenotype and tumor-infiltrating CD8+T cell-

mediated anti-tumor cell function.

CD8+ T cell Phenotypes of Interest

Cohoused mice provide an opportunity to investigate how microbial experience impacts

different T cell subsets. CD44 is a T cell surface marker that is upregulated and maintained on

both effector and memory T cells in response to TCR engagement or cytokine signaling (Baaten

et al., 2010). As such, cells that express high levels of CD44 (i.e. CD44^{hi}) were previously

activated and involved in an immune response. These cells are considered to be antigen-

experienced and have been shown to be elevated in cohoused mice (Beura et al., 2016). Tumor-

infiltrating CD8+ T cells have also been shown to be CD44^{hi} and elevated in cohoused mice

(Figure 4) during previous studies conducted in the Renkema lab (Groeber, 2020).
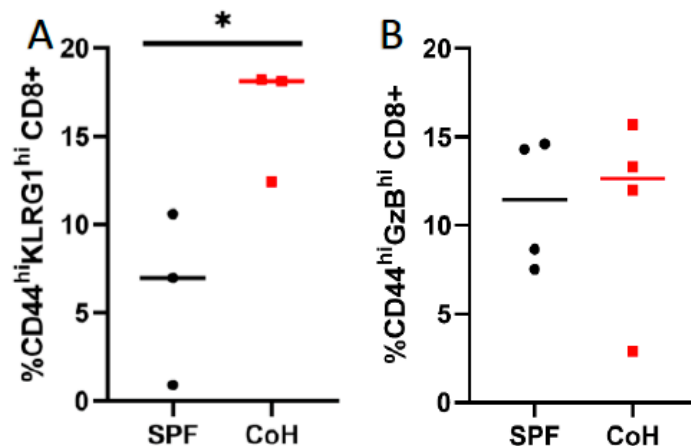
Figure 4: Tumor-infiltrating CD8+ T cells of CoH mice are more antigen experienced and differentiated.
Previous research conducted in the Renkema lab showed that CoH mice exhibit increased proliferation of antigen experienced tumor-infiltrating CD8+ T cells in response to B16 melanoma (Groeber, 2020).

KLRG1 is an indicator of terminal differentiation or senescence, and is expressed on long-lived effector cells (LLECs) after contraction of the primary immune response. LLECs provide long-term memory for viral infections as well as cancer, but exhibit reduced proliferative capacity when compared to other memory populations. KLRG1^{hi} cells are an intriguing therapeutic target, as their long-term protective functionality and ability to clear systemic infections may prove useful for CD8+ T cell vaccination development (Olson et al., 2013; Renkema et al., 2020). Investigating KLRG1 expression in a cohoused B16 tumor model will provide insight into the impact of microbial experience on generating LLECs.

Granzyme B (GzB), a serine protease that mediates apoptosis in target cells, will be measured and used as an indicator of effector function or cytotoxicity. GzB^{hi} CD8+ T cells are able to lyse infected or cancerous cells (Andersen et al., 2006; Mescher et al., 2006; Curtsinger et al., 2007). Without further stimulation, GzB^{hi} CD8+ T cells remain GzB^{hi} for a period of four weeks, and subsequent downregulation of GzB is indicative of a memory cell phenotype (Nowacki et al., 2007). Differences in cytotoxicity between SPF and CoH mice were inconclusive in previous work conducted in the Renkema lab (Figure 4B). Further study is required and will be conducted as part of this thesis.

PD-1/PD-L1 Axis Affects Anti-Tumor Immunity

Programmed cell Death-1 (PD-1) is an inhibitory protein receptor that is expressed on the surface of CD8+ T cells. PD-1 interacts with its ligand PD-L1, which is expressed on the surface of T and B cells, dendritic cells, macrophages, mesenchymal stem cells, mast cells, and tumor cells. PD-L1 expression is highly upregulated by inflammation, and binding of PD-L1 to PD-1 in

the presence of TCR activation inhibits proliferation, cytokine release, and cytotoxicity of T cells (Riella et al., 2012).

During a normal CD8+ T cell response, PD-1 is upregulated as a mechanism of peripheral tolerance in order to prevent autoimmunity. Studies using PD-1 knockout mice have shown increased susceptibility to autoimmune disease. One such study showed that non-obese diabetic (NOD) mice with a PD-1 knockout developed accelerated spontaneous diabetes, which occurred in 100% of male and female mice by 10 weeks (Keir et. al, 2006; Nishimura et. al, 2001).

Studies have also shown that PD-1 upregulation occurs rapidly during activation of naïve T cells. *In vitro* models have shown peak expression occurring in CD4+ T cells at 48 hours post-stimulation with anti-CD3/anti-CD28 (Yamazaki et. al, 2002), while *in vivo* models of viral LCMV-infection have shown peak expression of PD-1 in CD8+ T cells occurring at 72 hours (Ahn et. al, 2018).
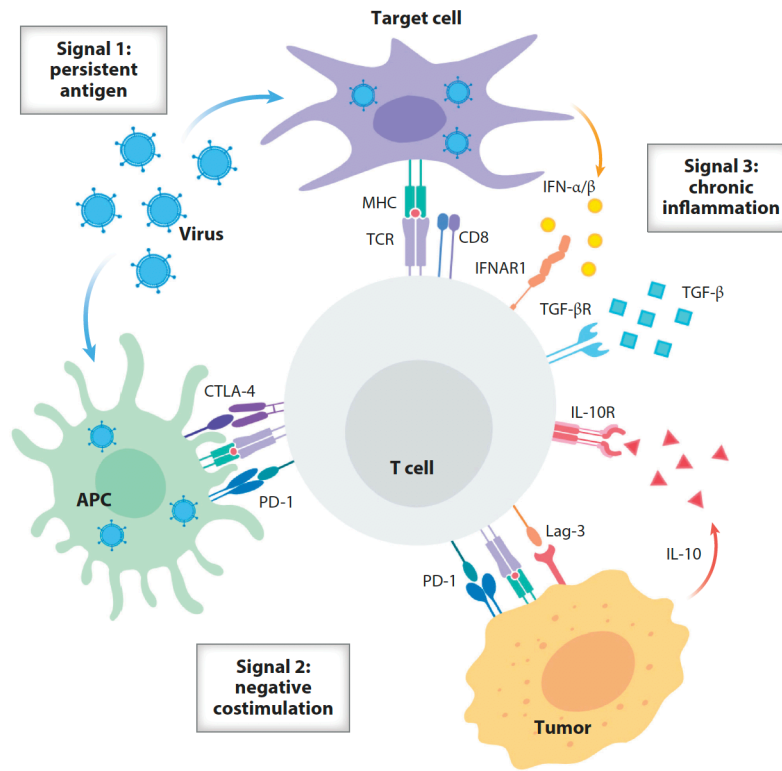
Figure 5: Three signal model of T cell exhaustion.
Chronic antigen stimulation leads to sustained coexpression of inhibitory receptors and their ligands. Inhibition of T cell effector function leads to chronic inflammation, as APC's and tumors secrete both proinflammatory and inhibitory cytokines. Chronic inflammation may also drive further T cell exhaustion (McLane et al., 2019).

The PD-1/PD-L1 interaction may function as a checkpoint to regulate immune responses, providing a safeguard against autoimmunity and immunopathology. This interaction allows the tumor cell to evade the immune response by inducing a downregulation in CD8+ T cell cytotoxicity. In the context of chronic antigen exposure, like cancer, continued stimulation of the PD-1/PD-L1 pathway leads to CD8+ T cell exhaustion and a loss of memory differentiation.

T cell exhaustion is characterized as the progressive loss of T cell effector function, sustained upregulation of multiple inhibitory receptors (ex. PD-1, CTLA-4, etc.), altered expression of key transcription factors, metabolic dysfunction, and a failure to acquire antigen-

independent memory T cell responsiveness. All of these changes lead to an inability to control tumor growth (Wherry & Kurachi, 2015). However, Ahn et. al showed that PD-1 expression is rapidly upregulated during activation of naïve CD8+ T cells, so knowing the timeframe since primary infection occurred is critical in differentiating between exhausted T cells and recently activated T cells. After a period of chronic antigen stimulation, increased PD-1 and CTLA-4 expression is indicative of T cell exhaustion, but reversal of this exhausted state is possible with targeted anti-PD-1 and anti-CTLA-4 immunotherapies (Robert et al., 2014; Wolchok et. al, 2017).

Additionally, chronic antigen stimulation may lead to a state of chronic inflammation and drive further T cell exhaustion (Figure 5) (McLane et al., 2019). The resulting decrease in anti-tumor immunity and impaired memory cell formation allows for the continued survival and proliferation of tumor cells.

Checkpoint Blockade

The first checkpoint blockade immunotherapy targeted the CTLA-4/B7 axis, which inhibits T cell effector function (Leach, Krummel, & Allison, 1996). During normal T cell activation, TCRs recognize antigen presentation on MHC-I and require co-stimulation of CD28 by B7 molecules expressed on cancer cells. Finally, cytokine stimulation with IL-2, IL-12, or type I interferons are needed for complete activation of T cell effector function. CTLA-4 is expressed on exhausted T cells and outcompetes CD28 for binding with B7. By interfering with CD28/B7 co-stimulation, CTLA-4 is able to inhibit T cell activation (Seidel et. al, 2018; Rudd et. al, 2009). Treatment with antibodies designed to bind CTLA-4 (anti-CTLA-4) prevents CTLA-

4/B7 binding and allows for appropriate CD28/B7 co-stimulation, which ultimately leads to T cell activation and cancer cell lysis (Leach, Krummel, & Allison, 1996).

More recently, checkpoint blockade immunotherapies have been developed to target the PD-1/PD-L1 axis. Administration of antibodies designed to bind PD-1 or PD-L1(anti-PD-1 & anti-PD-L1) interferes with binding, allowing the CD8+ T cell to retain its proliferative capacity and cytotoxicity. As a result, these treatments preserve the CD8+ T cells anti-tumor immunity leading to lysis of cancerous cells (Phan et al., 2003; Blank et al., 2004; Miller & Carson, 2020).

While these treatments have been effective, the nuances of their mechanisms remain incompletely characterized. In a phase 1 clinical trial of advanced melanoma patients whose disease had progressed after at least 2 doses of ipilimumab (anti-CTLA-4), treatment with intravenous pembrolizumab (anti-PD-1) had an overall response rate (ORR) of only 26% (Robert et al., 2014). However, in trials using combined nivolumab (anti-PD-1) and ipilimumab (anti-CTLA-4) therapy, an overall response rate of 55% was observed in treatment groups with <10% PD-L1 expressing tumors, compared to an ORR of 44% in the nivolumab group, and only 18% in the ipilimumab group (Wolchok et. al, 2017). It is worth noting that increases in ORR were consistent with increases in treatment-related adverse events. Discontinuation of therapy occurred more frequently in combination therapy than either monotherapy. The most common adverse events with potential immunologic causes were skin-related (rash, pruritis, etc.), while more severe adverse events were gastrointestinal in nature and resolved within 3-4 weeks. Only four deaths related to the study drugs were reported (Wolchok et. al, 2017).

Checkpoint blockade therapies have a favorable safety profile, but further investigation is needed to improve efficacy. We believe this plateau in efficacy may be due to the variability of the tumor microenvironment from one patient to the next. This heterogeneity may be due, in part,

to variation in effector memory CD8+ T cell subsets that have developed as a result of differing microbial experience from patient to patient. How microbial exposure affects the efficacy of checkpoint blockade immunotherapies can be investigated within a cohoused mouse model.

CHAPTER 3: METHODS

Mice Cohousing

A cohort of 50 female C57BL/6 specific pathogen-free mice was purchased from Charles River Laboratories (Mattawan, MI) for Cohort 6, and 30 female C57BL/6 SPF mice were purchased for Cohort 5. In both cohorts, the mice were split into groups of 4-5 mice per cage. Four cages with 5 SPF mice each served as control groups. Experimental mice were cohoused with female pet store mice purchased from Chow Hound (Holland, MI). All necessary precautions were taken to limit microbial exposure during handling, feeding, changing of supplies, and during weekly bleeds.

Mice were checked daily and fed ad libitum. Weekly cage cleaning was conducted according to a strict protocol to eliminate the risk of cross-contamination. SPF cages were always cleaned first to ensure no accidental introduction of pathogens from a previously cleaned CoH cage. Cages, lids, wires, and bottles were cleaned and soaked weekly with a solution of concentrated Clidox (1:3:1 dilution). Rescue disinfectant was also utilized to clean all housing supplies.

CoH and SPF cages were kept in a satellite-vivarium separate from all other research animals at Grand Valley State University. All animals were used in accordance with the guidelines of the Institutional Animal Care and Use Committee (IACUC) at Grand Valley State University (Protocol Number: 19-08-A).

Pathogen Testing

Fecal and blood samples were collected on day 0 from PS mice and after day 30 from SPF and CoH mice. Samples were pooled for collection from each cage and sent to Charles

River Laboratories to test for specific pathogens (CR-RADS). The "pooling" method was used to generate a representative sample of all mice in each individual cage.

Blood Collection & Analysis

Mice were briefly anesthetized with isoflurane and bled retro-orbitally once per week during the cohousing period. Samples for flow cytometry preparation were stored in heparinized tubes. Red blood cells were lysed with 300 μL ACK lysis buffer (KD Medical), vortexed, and incubated at room temperature for 3 minutes. 1,000 μL PBS was added to dilute and deactivate the ACK lysis buffer, and the samples were centrifuged for 4 minutes at 4,000 RPM. For flow cytometry preparation, the cell pellet was incubated after staining with antibody panels 1-3 (Table 2) and fixed with a FoxP3 Fix/Perm kit (Tonbo Biosciences).

Blood samples intended for serum collection were stored in non-heparinized tubes, which allowed the blood to clot. Samples were centrifuged for 8 minutes at 8,000 RPM. 30 μL of serum was pipetted into Eppendorf tubes and stored at -80 °C for future analysis.

B16-F10 Melanoma Cell Culture & Injection

B16-F10 cells (ATCC) were cultured in RPMI 10% complete medium (RPMI + 10% FBS + 5,000 μg/L Streptomycin + 5,000 U/mL Penicillin + 50 μM 2-mercaptoethanol). 2.5 x 10^5 B16 cells in 200 μL PBS was injected subcutaneously into the left and right shaved flanks of each experimental mouse. The mice were anesthetized with isoflurane to limit distress experienced during the procedure. In accordance with the lab IACUC protocol (19-08-A), the mice were euthanized by day 14, when necrosis developed, or when the tumors reached a size of 10 mm^3.

Tissue Collection & Processing

Mice were euthanized with a lethal dose of isoflurane and secondary cervical dislocation. Blood was collected for flow cytometry preparation and serum collection according to the methods described above. Spleens, draining lymph nodes (inguinal), and B16 melanoma tumors were collected in 3 mL RPMI-2% FBS. Tumors were collected from the right and left flanks of each mouse and stored individually in pre-weighed conicals of 3 mL RPMI-2% FBS. Tumor weights were determined using a VWR 123P analytical balance, after which, left and right tumors were combined and processed into single cell suspension. Spleen samples were treated with 300 μL ACK lysis buffer (KD Medical), vortexed, incubated at room temperature for 1 minute, and 1,000 μL PBS was added to dilute and deactivate the ACK lysis buffer. All samples were washed with FACS buffer (1x PBS + 1% FBS), resuspended in FACS buffer, and incubated for 20 minutes at 4 °C after appropriate antibody staining (Table 2).

1 mL of tumor supernatant was collected and stored at -80 °C for future analysis. Tumor samples were resuspended in 15 mL RPMI-2% FBS and underlaid with 10 mL Ficoll-Paque PLUS (Cytiva). The tumor sample was then centrifuged at 800 G with no brakes for 20 minutes at room temperature to separate tumor-infiltrating white blood cells from tumor cells. The liquid layer containing white blood cells was decanted and centrifuged at 1500 RPM for 5 minutes, resuspended in 1 mL FACS buffer, and prepped for flow cytometry. Tumor pellets were resuspended in 2-5 mL FACS buffer, prepped for analysis by flow cytometry, and used for *in vitro* checkpoint blockade assays.

In vitro **T cell Stimulation**

Cells from spleen and tumor samples were cultured in 24-well plates pre-coated with 20 μg/mL anti-CD28 and 10 μg/mL anti-CD3 to stimulate T cell activation. The cells were cultured in RPMI 10% complete medium (RPMI + 10% FBS + 5,000 μg/L Streptomycin + 5,000 U/mL Penicillin + 50 μM 2-mercaptoethanol), and 10 U/mL IL-2 was added to support T cell survival. Cell preparations were stained on day 3 post-culture with various combinations of antibodies (Tonbo Biosciences, unless otherwise noted) for CD4, CD8, CD44, CD69, Granzyme B (Biolegend), and Live/Dead Fixable Red cell stain kit (Thermo Fisher) and analyzed by flow cytometry. Supernatant was collected for future ELISA analysis.

Table 1: Antibody panels used for *in vitro* T cell stimulation

Panel 1: T cell Activation Culture #1				Dilution
CD8	PerCp-Cy5.5	Tonbo	65-1886-U025	1:400
CD44	FITC	Tonbo	35-0441-U025	1:500
CD69	PE-Cy7	Tonbo	60-0691-U025	1:400
Live/Dead Red	PE	Thermo Fisher	L34971	1 uL per mL
Panel 2: T cell Activation Culture #2				Dilution
CD8	PerCp-Cy5.5	Tonbo	65-1886-U025	1:400
CD69	PE-Cy7	Tonbo	60-0691-U025	1:400
Live/Dead Red	PE	Thermo Fisher	L34971	1 uL per mL
Granzyme B	FITC	Biolegend	515403	2.5 uL per sample

In vitro **Checkpoint Blockade Assay**

Standard culture preparation protocols were followed as outlined above (*in vitro* T cell stimulation). Single cell suspensions of spleen and tumor samples were counted and diluted with additional RPMI 10% complete medium to achieve 2.0×10^6 cells per mL (spleen) and 2.4×10^5 cells per mL (tumor). All experimental conditions (+Tumor, anti-PD-1, and anti-PD-1/anti-

CTLA-4) received 100 μL analogous tumor cells in each well. Spleen samples received no analogous tumor cells. Checkpoint blockade conditions received 10 μg/mL anti-PD-1 (Tonbo Biosciences) or a combination treatment of 10 μg/mL anti-PD-1 (Tonbo Biosciences) & 10 μg/mL anti-CTLA-4 (Tonbo Biosciences). Cell preparations were stained on day 3 with antibody panels listed in Table 1 and analyzed by flow cytometry.

Ex vivo **Flow Cytometry Analysis**

Spleen, draining lymph nodes, blood, and B16 melanoma tumors were harvested and prepped for *ex vivo* flow cytometry analysis using a Beckman & Coulter CytoFlex 4-channel flow cytometer. Samples were resuspended in 200 μL FACS buffer (1x PBS + 2% FBS) and run at a speed of 1,000-5,000 events per second for $\geq$ 2 minutes. All samples were fixed with a Fix/Perm FoxP3 kit (Tonbo Biosciences) and stained for intracellular enzymes like Granzyme B. T cells were surface stained with panels of antibodies listed in Table 1 & 2 (intracellular antibodies highlighted light blue).

Statistical Analysis

Flow cytometry data were acquired on the preinstalled CytExpert software (Beckman & Coulter) and analyzed using FlowJo 10.7.1 (Tree Star Inc). Graphing and statistical analysis was done in Prism 8 (GraphPad). Significance was determined by p-values < 0.05 using an unpaired Student's t-test, Multiple t-tests, or Two-Way ANOVA with Bonferroni or Tukey's multiple comparison test.

Table 2: Antibody panels used for *ex vivo* flow cytometry analysis of blood, spleen, draining lymph nodes, tumor, and tumor pellet analysis.

Panel 1: T cell activation				Dilution
CD4	PE	Tonbo	50-0041	1:400
CD8	PerCp-Cy5.5	Tonbo	65-1886	1:400
CD44	FITC	Tonbo	35-0441	1:500
KLRG1	PE-Cy7	Biolegend	138415	1:400
Panel 2: T cell and NK cell cytotoxicity				
CD8	PerCp-Cy5.5	Tonbo	65-1886	1:400
NK1.1	PE	Tonbo	50-5941	1:400
KLRG1	PE-Cy7	Biolegend	138415	1:400
Granzyme B	FITC	Biolegend	515403	2.5μL per sample
Panel 3: T cell inhibition				
CD8	PerCp-Cy5.5	Tonbo	65-1886	1:400
KLRG1	PE-Cy7	Tonbo	35-5893	1:400
PD-1 (CD279)	PE	Tonbo	50-9985	1:400
Granzyme B	FITC	Biolegend	515403	2.5μL per sample
Panel 6: Tumor Phenotype				
CD133	PE-Cy7	Biolegend	141209	1:400
PD-L1	PerCp-Cy5.5	Biolegend	124333	1:400
CD45	FITC	Biolegend	103107	1:400
Ki67	PE	Biolegend	151209	1:200

CHAPTER 4: RESULTS

CoH mice contract pathogens after 30 days of cohousing with pet store mice

Researchers at the University of Minnesota have shown that cohousing SPF mice with PS mice induces effector-differentiated memory T cell populations within genetically homogenous C57BL/6 mice (Beura et. al, 2016). While this type of mouse husbandry is normally conducted under biosafety-level 3 (BSL-3) conditions, we show here that it is possible to maintain the pathogen-free state of SPF mice while generating CoH mice under biosafety-level 2 (BSL-2) conditions.

SPF mice were purchased from Charles River Laboratories (Mattawan, MI) and arrived with a day 0 pathogen screening. To confirm transfer of pathogens from PS mice to CoH mice, blood and stool samples were taken from PS mice on day 0 and additional samples were taken from SPF and CoH mice on day 30 of cohousing. Samples were pooled by cage to provide a more complete understanding of the pathogens present within each group. Reports from Charles River Research Animal Diagnostic Services (CR-RADS) confirm that PS mice are infecting CoH mice with many common murine pathogens by day 30 of cohousing (Table 3). The most commonly transferred pathogens are viruses such as Theiler's murine encephalomyelitis virus (GDVII), mouse norovirus (MNV), mouse adenovirus 1 & 2 (MAV), and mouse parvovirus 3 (MPV-3). Additionally, our data show that various species of pinworm and the bacterium *Mycoplasma pulmonis* have also successfully transferred from PS to CoH mice. These findings remain consistent with the pathogen screening conducted by Beura et al.

Table 3: Cohousing SPF with PS mice generates microbially experienced CoH mice by d30.

	Percent of Mice Testing Positive for Pathogen		
VIRUS	**Day 0 SPF**	**Day 0 PS**	**Day 30 CoH**
Sendaivirus (SEND)	0	78	0
Pneumonia virus of mice (PVM)	0	33	0
Mouse hepatitis virus (MHV)	0	100	44
Minute Virus of Mice (MVM)	0	100	11
Mouse Parvovirus 1 (MPV-1)	0	100	0
Mouse Parvovirus 2 (MPV-2)	0	78	0
Mouse Parvovirus 3 (MPV-3)	0	86	56
Mouse Parvovirus 4 (MPV-4)	0	0	0
Parvovirus NS-1 (NS-1)	0	89	11
Mouse norovirus (MNV)	0	63	78
Theiler's murine encephalomyelitis virus (GDVII)	0	89	100
Reovirus (REO)	0	0	0
Mouse rotavirus (EDIM; ROTA-A)	0	44	0
Lymphocytic choriomeningitis virus (LCMV)	0	11	0
Ectromelia virus (ECTRO)	0	0	0
Mouse adenovirus 1 & 2 (MAV)	0	100	78
Mouse cytomegalovirus (MCMV)	0	0	0
Mouse pneumonitis virus (K)	0	0	0
Mouse thymic virus (MTLV)	0	0	0
Polyoma virus (POLY)	0	0	0
Hantaan (HANT)	0	0	0
Prospect Hill Virus (PHV)	0	0	0
Lactate dehydrogenase-elevating virus (LDV)	0	0	0
BACTERIA	**Day 0 SPF**	**Day 0 PS**	**Day 30 CoH**
Mycoplasma pulmonis **(MPUL)**	0	89	11
Cilia-associated respiratory bacillus (CARB)	0	0	0
Clostridium piliforme **(CPIL)**	0	57	0
Corynebacter bovis	0	0	0
PARASITES/PROTOZOA/FUNGI	**Day 0 SPF**	**Day 0 PS**	**Day 30 CoH**
Encephalitozoon cuniculi **(ECUN)**	0	44	0
Mites	0	14	0
Pinworms	0	43	44
Aspiculuris tetraptera (pinworm)	0	14	11
Syphacia muris (pinworm)	0	0	0
Syphacia obevelata (pinworm)	0	29	44

Between days 7 and 14 of cohousing with PS mice, CoH mice appeared visibly ill as evidenced by a lack of appetite, decreased grooming habits, and lethargy. These symptoms typically resolve between days 21 and 28 during contraction of the primary immune response.

Beura et. al observed a 22% mortality rate in the first 8 weeks of cohousing. Our mortality rates in cohort 5 and 6 were 28% and 10%, respectively.

The cohousing model was implemented in the Renkema lab at Grand Valley State University in 2019. Since that time, six cohorts of 25-50 mice each have been successfully cohoused. Through the use of a BSL-2 satellite vivarium and strict hygiene protocols, we show here that it is possible to generate CoH mice with levels of microbial exposure consistent with the data reported by Beura et al.

CoH mice are more antigen-experienced and differentiated after cohousing period

Both SPF and CoH mice were bled weekly during the cohousing period in order to investigate the impact of microbial exposure on antigen experience and differentiation of CD8+ T cell populations. Weekly bleeds were conducted with 4-5 mice from both SPF and CoH groups on day 7, 14, 21, and 28. Blood samples were stained with antibody panels 1-3 (Table 2) and analyzed via flow cytometry. FlowJo software was used to determine the percentage of CD44^{hi}KLRG1^{hi} CD8+ T cells in SPF and CoH mice. This phenotype was used as an indicator of antigen experience (CD44) and differentiation (KLRG1). A consistent gating strategy was applied to all weekly bleed data (Figure 6).

By day 14 of cohousing in both cohort 6, CoH mice had a significantly higher percentage of CD44^{hi}KLRG1^{hi} CD8+ T cells compared to SPF mice (Figure 7B). This phenotype of CD8+ T cells increases in CoH mice until approximately day 21 of cohousing where the frequency begins to plateau, presumably during the contraction phase of immunity. The observed plateau in this CD8+ T cell population is reported to persist for approximately 70 days (Beura et. al, 2016).
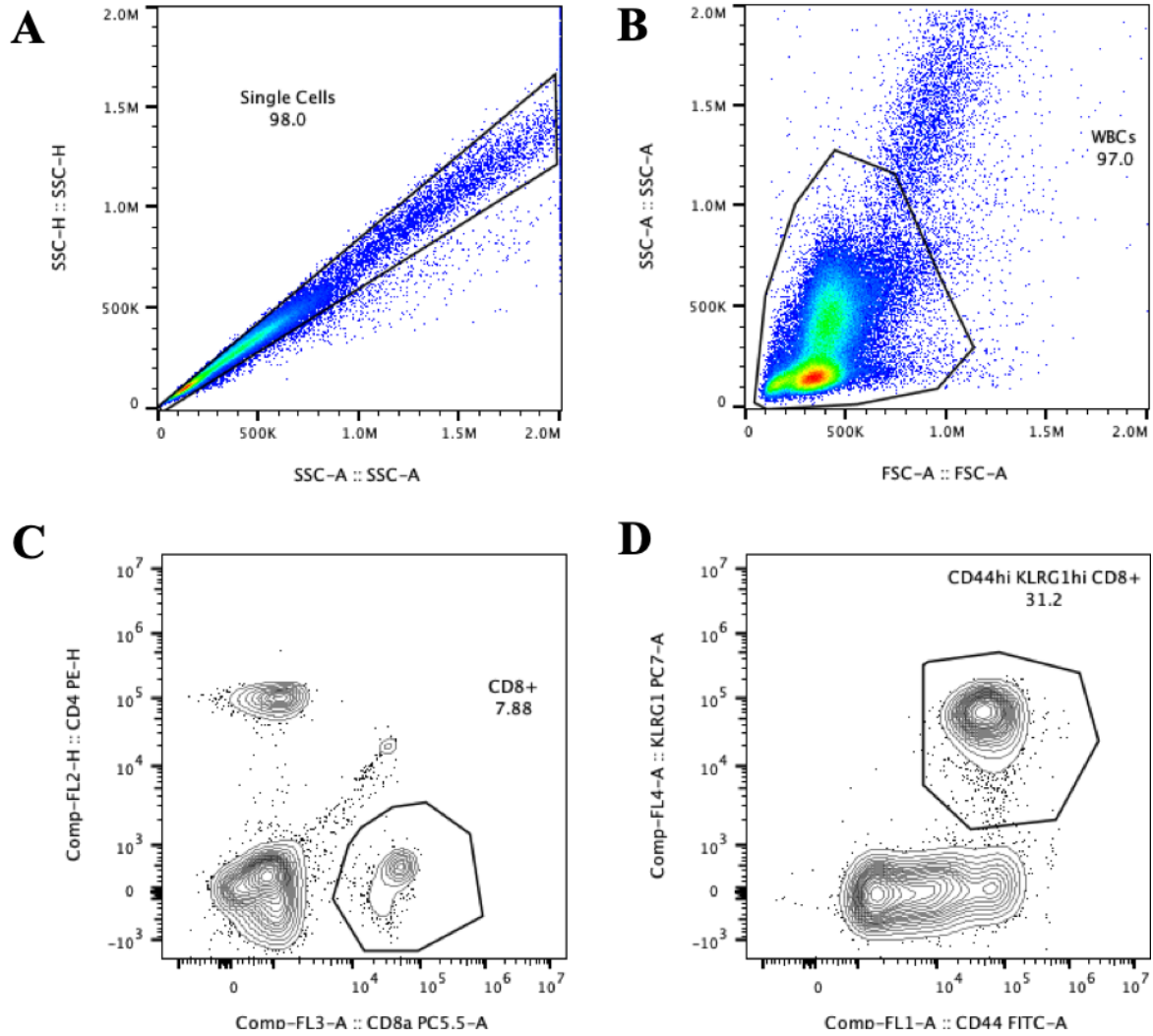
Figure 6: CD44^hiKLRG1^hi CD8+ gating strategy for weekly bleeds and harvest samples of dLN, spleen, and tumor.
FlowJo was used to gate populations of CD44^hiKLRG1^hi CD8+ T cells in CoH and SPF mice during weekly bleeds and on blood samples from harvests. (**A**) Single cells were obtained on side-scatter area (SSC-A) by side-scatter height (SSC-H). (**B**) White blood cells (WBCs) were gated on forward-scatter area (FSC-A) by side-scatter area (SSC-A). (**C**) CD8+ T cells were differentiated based on high expression of CD8 and low expression of CD4. (**D**) Gates for high expression of both CD44 and KLRG1 were drawn to differentiate CD44^hiKLRG1^hi populations of CD8+ T cells. Gating strategy was identical for all timepoints during cohousing and for all harvest blood samples. Mouse CoH 6-2 from d28 weekly bleed in Cohort 6 is used as an example above.

The near absence of CD44^{hi}KLRG1^{hi} CD8+ T cells in SPF mice during the entire period of cohousing is a significant and critical indication that the SPF mice have remained pathogen-free. These results are consistent with previous cohorts conducted in the Renkema lab (Groeber, 2020), and provides confirmation that the impact of microbial experience can be reliably elucidated in further experiments using these SPF mice as controls.
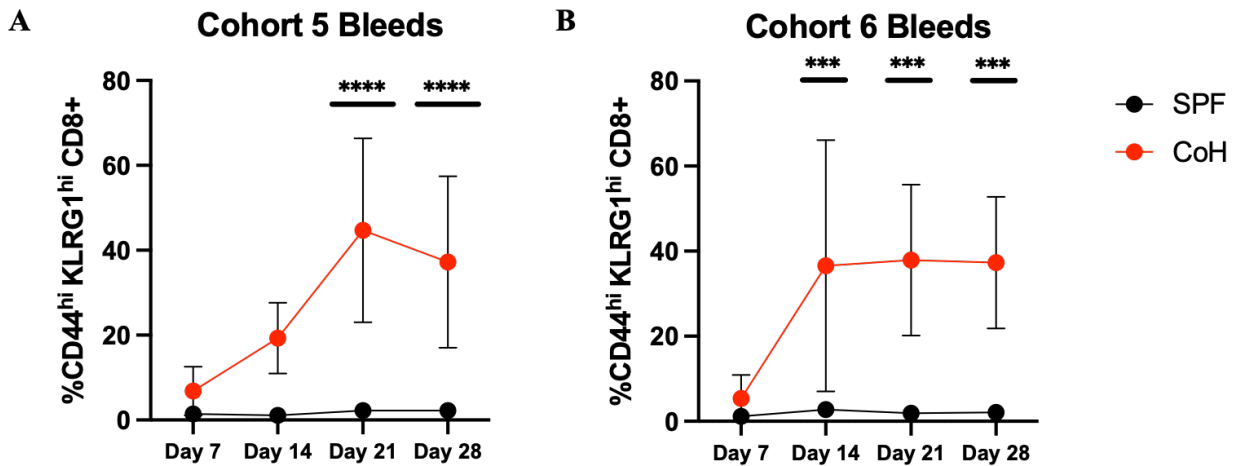
Figure 7: CoH mice have significantly increased CD44^{hi}KLRG1^{hi} CD8$^+$ T cell populations after 28 days of cohousing.
Weekly bleeds were conducted with 5-6 mice from both SPF and CoH populations. By day 21, cohoused mice had developed significantly increased CD44^{hi}KLRG1^{hi} CD8$^+$ T cell populations in Cohort 5 (**A**) and significant increases were observed by day 14 in Cohort 6 (**B**), indicating increased antigen-experience and differentiation. SPF mice exhibited little to no CD44^{hi}KLRG1^{hi} CD8$^+$ T cell populations, confirming their pathogen-free state. Data points represent the mean of N = 5 mice in Cohort 5 and N = 6 mice in Cohort 6 for both SPF and CoH groups. Two-way ANOVA with Bonferroni was used to determine statistical significance.

CD8+ T cells from Blood, Spleen, dLN, and Tumor in CoH mice are more antigen-experienced and differentiated after B16-melanoma

All SPF and CoH mice received subcutaneous injections of B16 melanoma cells in both the right and left shaved flanks on day 30 of cohousing. Tumor formation was visible and palpable in all mice when euthanized on day 10 post-injection. Blood, spleen, draining lymph nodes, and tumors were harvested from every mouse. All tissues were stained with antibody panels 1-3 (Table 2) and prepped for analysis by flow cytometry. *Ex vivo* tissue samples were gated with the same strategy utilized for weekly bleeds (Figure 6).

Blood samples of CoH mice exhibited increased percentage of CD44^{hi}KLRG1^{hi} CD8+ T cells compared to SPF mice (Figure 8A). This result is consistent with the data presented for weekly bleeds in Figure 7. However, an overall increase of approximately 10% in the frequency of CD44^{hi}KLRG1^{hi} CD8+ T cells in CoH mice is observed when comparing d28 of cohousing (pre-melanoma injection) to d10 post-melanoma injection.

Spleen samples of CoH mice also show significantly increased percentage of CD44^{hi}KLRG1^{hi} CD8+ T cells compared to SPF mice (Figure 8B), and at levels comparable to blood samples (Figure 8A). The tumor-draining lymph nodes of CoH mice also show significantly increased percentage of CD44^{hi}KLRG1^{hi} CD8+ T cells compared to SPF mice (Figure 8C), however, overall frequency of this population in dLNs is quite low compared to all other tissue types.

CoH mice had an increased percentage of CD44^{hi}KLRG1^{hi} tumor-infiltrating CD8+ T cells compared to SPF mice (Figure 8D). CD44^{hi}KLRG1^{hi} CD8+ T cell populations observed after 30 days of cohousing are considered LLECs. LLECs are long lived effector cells that exhibit increased KLRG1 expression after contraction. This population of LLECs was nearly absent in the blood, spleen, and dLN of SPF mice. However, nearly 70% of tumor-infiltrating

CD8+ T cells in SPF mice are also CD44^{hi}KLRG1^{hi}, suggesting a key role for LLECs in the

intratumoral immune response to melanoma. These results are consistent with previous findings

from the Renkema lab (Groeber, 2020), and were repeated two times throughout cohorts 5 and 6.
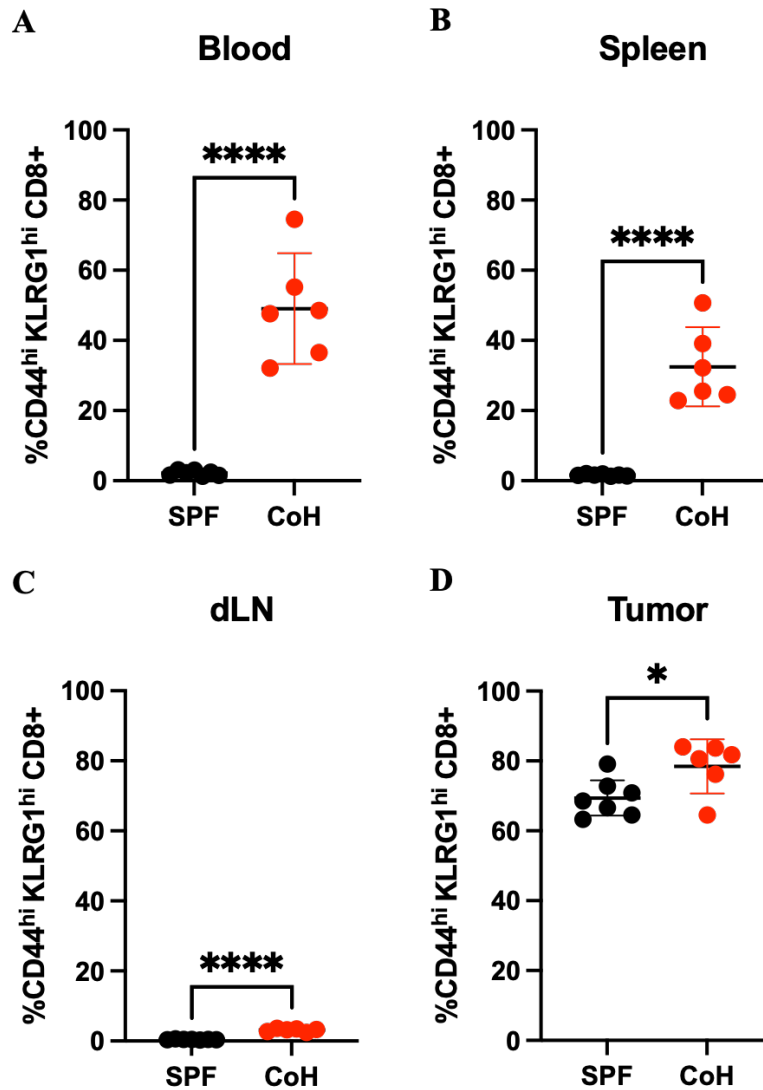
Figure 8: CoH mice have significantly increased CD44^{hi}KLRG1^{hi} CD8^{+} T cells in blood, spleen, dLN, and tumor after B16 melanoma injection.
CoH mice exhibited significantly increased percentages of antigen-experienced and differentiated CD8+ T cells in blood (**A**), spleen (**B**), dLN (**C**), and tumor (**D**) at d10 post-injection. Data are shown for Harvest 2 of Cohort 6 with N = 7 SPF mice and N = 6 CoH mice. Results repeated 2 times. Statistical significance was determined by unpaired t-test.

CoH mice are more cytotoxic in *ex vivo* blood, dLN, spleen, and tumor after cohousing and B16-melanoma injection

We have shown that CoH mice are more antigen-experienced and differentiated after 28 days of cohousing, and have also shown that CD44^{hi}KLRG1^{hi} CD8+ T cell populations in CoH mice increase further by day 10 post-melanoma injection. To better understand differences in effector function between SPF and CoH mice, we stained weekly blood and *ex vivo* tissue samples for the intracellular enzyme Granzyme B (Table 2, Panel 2). FlowJo software was used to determine the percentage of GzB^{hi} CD8+ T cells in SPF and CoH mice. A consistent gating strategy was applied to all weekly bleed and *ex vivo* tissue data (Figure 9).

CoH mice undergo significant increases in GzB^{hi} CD8+ T cell populations throughout the cohousing period, while the presence of this same effector population remains nearly absent in SPF mice. The proportion of GzB^{hi} CD8+ T cells peaks around 40% by day 14 of cohousing (Figure 10). Consistent with the observed contraction of CD44^{hi}KLRG1^{hi} CD8+ T cells (Figure 7), we see a similar trend by day 21 in GzB^{hi} CD8+ T cells of CoH mice (Figure 10). Both observations are consistent with normal contraction of the immune response.

Blood, spleen, dLN, and tumor tissues were all harvested 10 days post-melanoma injection for *ex vivo* analysis. GzB^{hi} CD8+ T cell populations were significantly higher in CoH mice in all tissue types (Figure 11). The proportion of GzB^{hi} tumor-infiltrating CD8+ T cells in CoH mice was nearly twofold greater than the proportion observed in SPF mice (Figure 11D). This result was repeated 3 times in *ex vivo* tissue samples.
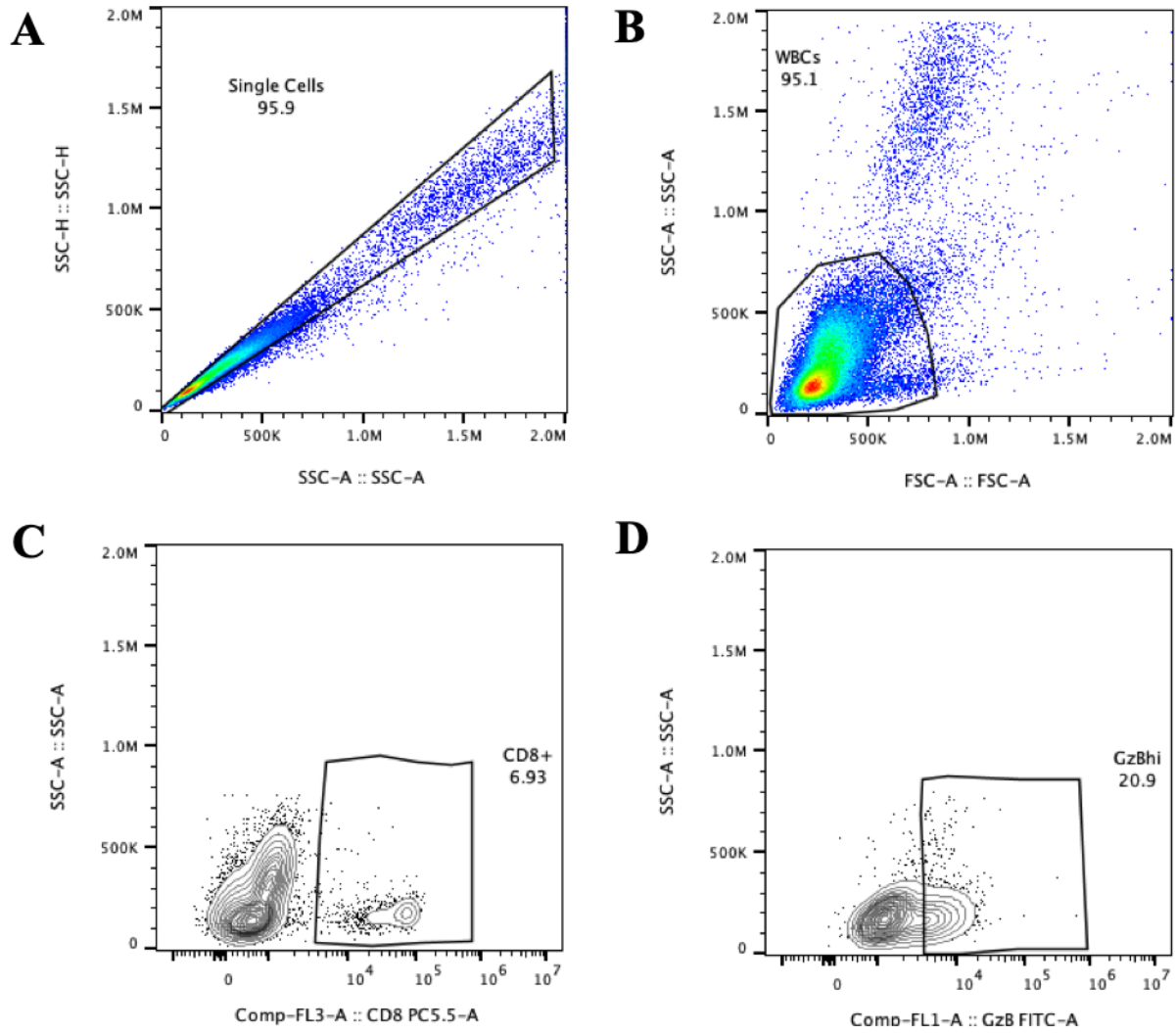
Figure 9: GzB^{hi} CD8⁺ gating strategy for weekly bleeds and harvest samples.
FlowJo was used to gate populations of GzB^{hi} CD8$^+$ T cells in CoH and SPF mice from
weekly bleeds and tissues from harvest. (**A**) Single cells were obtained on side-scatter
area (SSC-A) by side-scatter height (SSC-H). (**B**) White blood cells (WBCs) were gated
on forward-scatter area (FSC-A) by side-scatter area (SSC-A). (**C**) Distinct populations
of CD8+ T cells were differentiated based on high expression of CD8 against side-scatter
area (SSC-A). (**D**) Gates for GzB^{hi} CD8$^+$ T cell populations were drawn on GzB by side-
scatter area (SSC-A). Gating strategy was identical for all timepoints during cohousing
and for all tissue harvests. Blood sample from mouse CoH 6-1 in Harvest 2 of Cohort 6 is
shown above.

Previous results reported from the Renkema lab indicated that GzB expression was elevated in CD8+ T cell populations of CoH mice in blood and spleen samples after a 30-day cohousing period (Groeber, 2020). Here, we are able to confirm those results in blood samples after 28 days of cohousing (Figure 10). We did not harvest any mice on day 28, so post-cohousing GzB expression in the spleen was not an observable endpoint. We did, however, build upon Groeber's findings by showing increased GzB expression in CD8+ T cells of CoH mice in blood, spleen, dLN, and tumor samples after challenge with B16 melanoma (Figure 11).
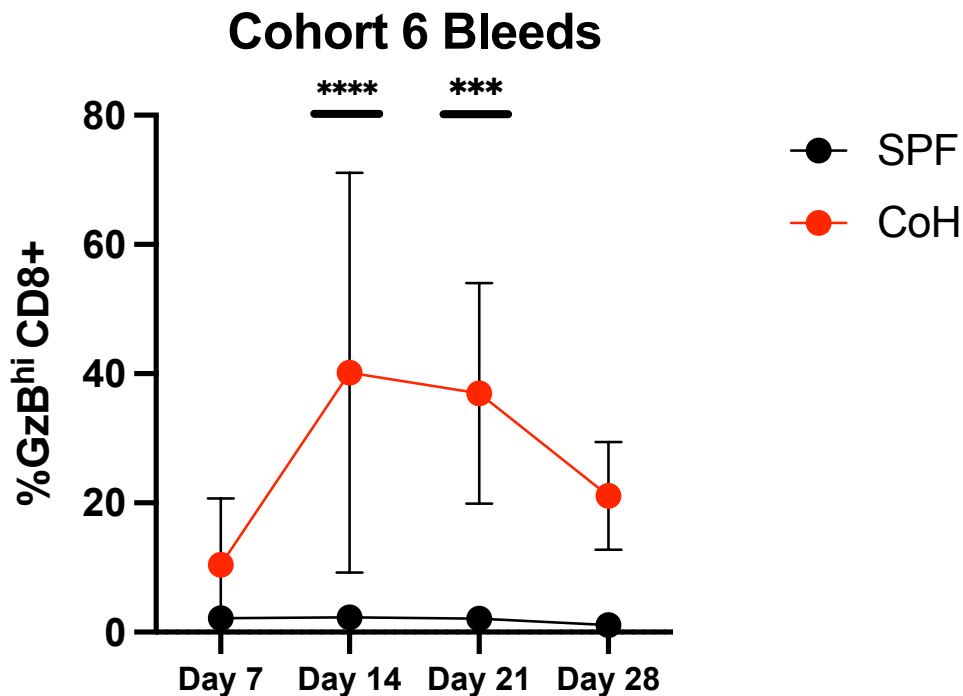
Figure 10: Granzyme B expression is significantly higher in CD8+ T cells of CoH mice throughout 28 days of cohousing.
CD8+ T cells of CoH mice exhibited significantly increased GzB^{hi} populations throughout the 28-day cohousing period. Data points represent the mean of N = 6 mice for both SPF and CoH groups. Two-way ANOVA with Bonferroni was used to determine statistical significance. Results were repeated 2 times.
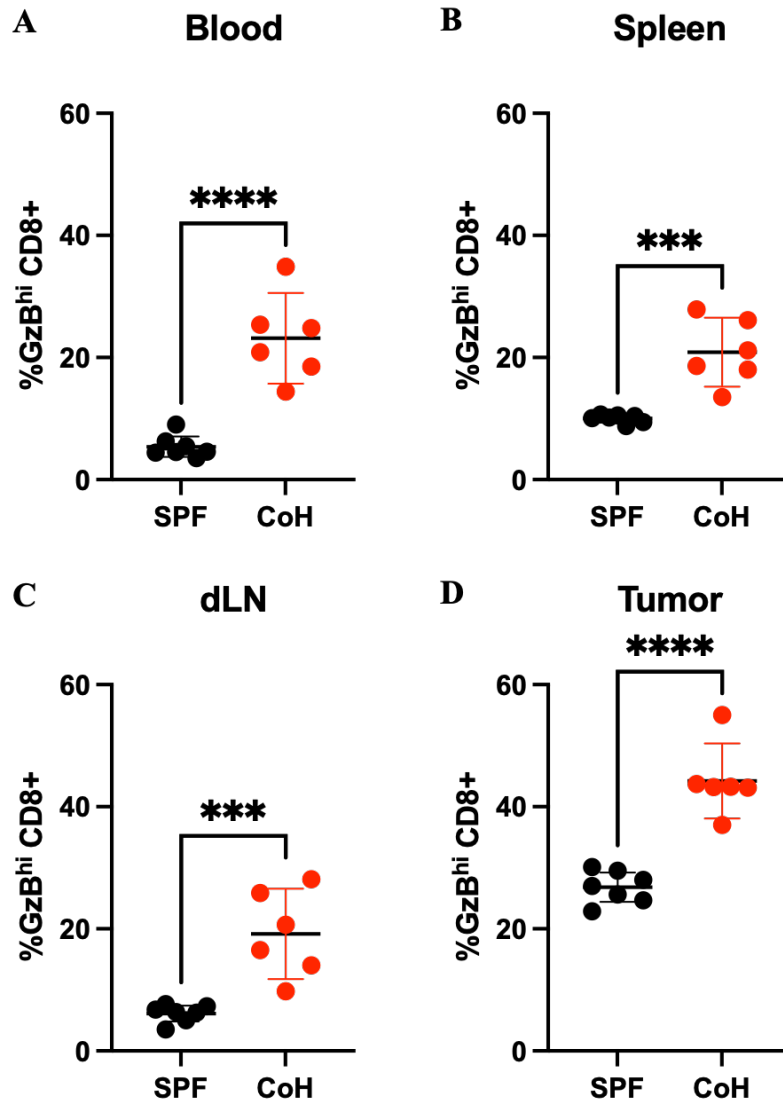
Figure 11: CoH mice have significantly increased GzB^hi CD8^+ T cells in blood, spleen, dLN, and tumor after B16 melanoma injection.
CoH mice exhibited significantly increased percentages of Granzyme B expressing CD8+ T cells in blood (**A**), spleen (**B**), dLN (**C**), and tumor (**D**) at d10 post-injection. Data are shown for Harvest 2 of Cohort 6 with N = 7 SPF mice and N = 6 CoH mice. Results repeated 3 times. Statistical significance was determined by unpaired t-test with all p-values < 0.01

Tumor-infiltrating CD8⁺ T cells of CoH mice are more cytotoxic than SPF mice after *in vitro* stimulation

Here, we confirm our *ex vivo* findings of increased GzB expression in tumor-infiltrating CD8+ T cells of CoH mice by conducting an *in vitro* stimulation. Conducting in vitro assays provides greater control of environmental conditions and allows for a more accurate characterization of SPF and CoH CD8+ T cells. To stimulate T cell activation, 24-well plates were coated with anti-CD28 and anti-CD3 antibodies and incubated overnight. IL-2 was added to provide signal 3 for full T cell activation. Density gradient centrifugation was used to purify the tumor-infiltrating white blood cells from the melanoma tumor cells before initiation of cell culture. After 3 days of incubation, 1 mL of supernatant was collected from each well and stored for future ELISA analysis. Culture samples were stained with antibody panels 1-2 (Table 1) and flow cytometry analysis was conducted. FlowJo software was used to determine the percentage of GzB^{hi} CD8+ T cells in SPF and CoH mice 3 days after *in vitro* stimulation. A consistent gating strategy was applied to all *in vitro* stimulation data (Figure 12).

CoH mice exhibit an increased proportion of GzB^{hi} CD8+ T cells 3 days after *in vitro* stimulation (Figure 13). This result was repeated 2 times, and suggests that CoH mice possess tumor-infiltrating CD8+ T cell populations that are capable of a more cytotoxic immune response upon *in vitro* stimulation.
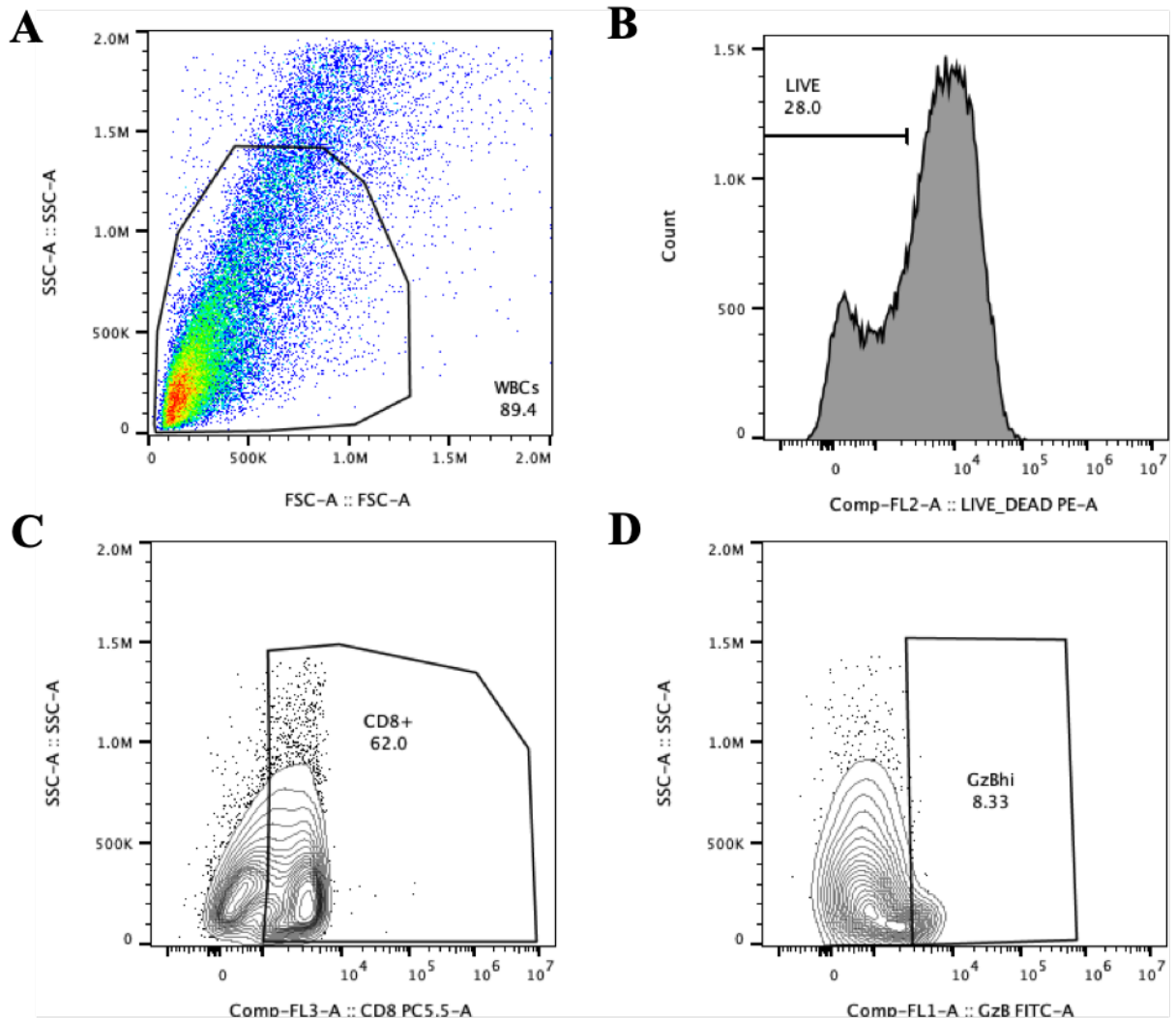
Figure 12: Gating strategy for *in vitro* cell cultures of GzB^hi tumor-infiltrating CD8+ T cells.

FlowJo was used to gate populations of tumor-infiltrating GzB^{hi} CD8$^+$ T cells in CoH and SPF mice from cell cultures. (**A**) White blood cells (WBCs) were gated on forward-scatter area (FSC-A) by side-scatter area (SSC-A). (**B**) Live cells were gated by histogram of Live/Dead fluorescence intensity. (**C**) Distinct populations of CD8+ T cells were differentiated based on high expression of CD8 against side-scatter area (SSC-A). (**D**) Gates for GzB^{hi} CD8$^+$ T cell populations were drawn on GzB by side-scatter area (SSC-A). Gating strategy was identical for all cell cultures. Sample from Harvest 1 of Cohort 6 is shown above.

Figure 13: Tumor-infiltrating CD8+ T cells of CoH mice have increased Granzyme B expression on day 3 after *in vitro* stimulation.
Tumor-infiltrating CD8+ T cells were stimulated with anti-CD28, anti-CD3, and IL-2. Cultures were analyzed on day 3 post-stimulation. CoH mice exhibit significantly higher proportions of GzB^{hi} CD8+ T cells after stimulation. (A) Data shown for Cohort 6, Harv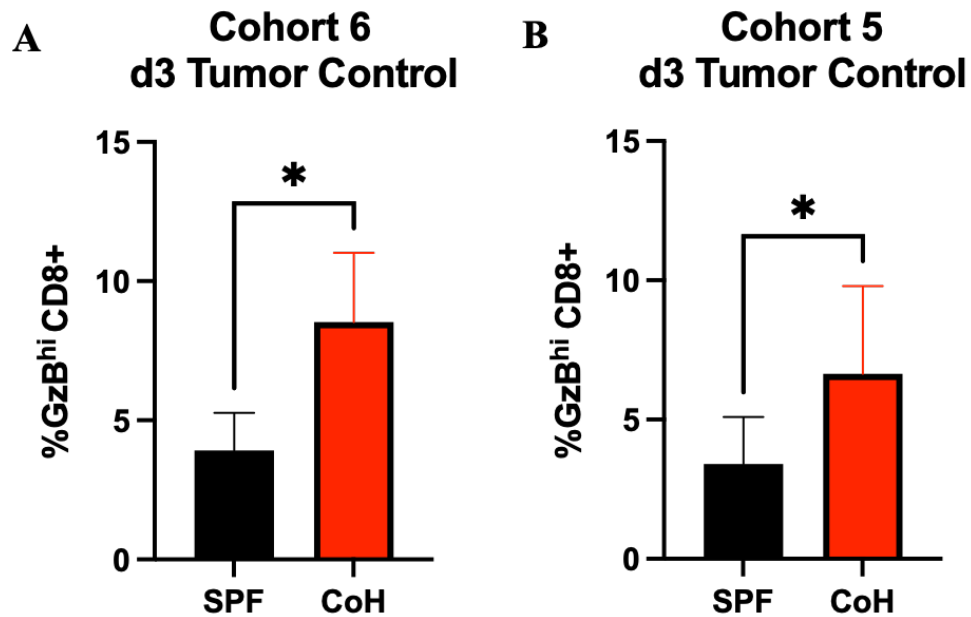est 1; N = 3 mice per group. (B) Data shown for Cohort 5, Harvest 2; N = 3 mice per group. Statistical significance determined by unpaired t-test with p-values < 0.05

CoH mice have significantly smaller tumors by weight than SPF mice

B16 melanoma was injected into the shaved right and left flanks of all mice and tumors were harvested 10 days later. Right and left tumors were stored in individual conicals and immediately weighed. SPF tumors were visibly larger than CoH tumors, and evidence of increased angiogenesis was apparent to the naked eye (Figure 22, Appendix).

We observed that SPF mice have significantly larger tumors by weight when compared to CoH mice (Figure 14). These results were repeated in both Cohort 5 and Cohort 6. Further investigation is needed to determine if this difference in tumor weight is time-dependent after injection of B16 melanoma. Here, we show data for 10 days post-injection, but investigating growth at timepoints beyond 10 days would provide insight into the durability and longevity of

this anti-tumor growth response in CoH mice. Future experiments will be able to determine whether or not microbial exposure improves long-term tumor control.
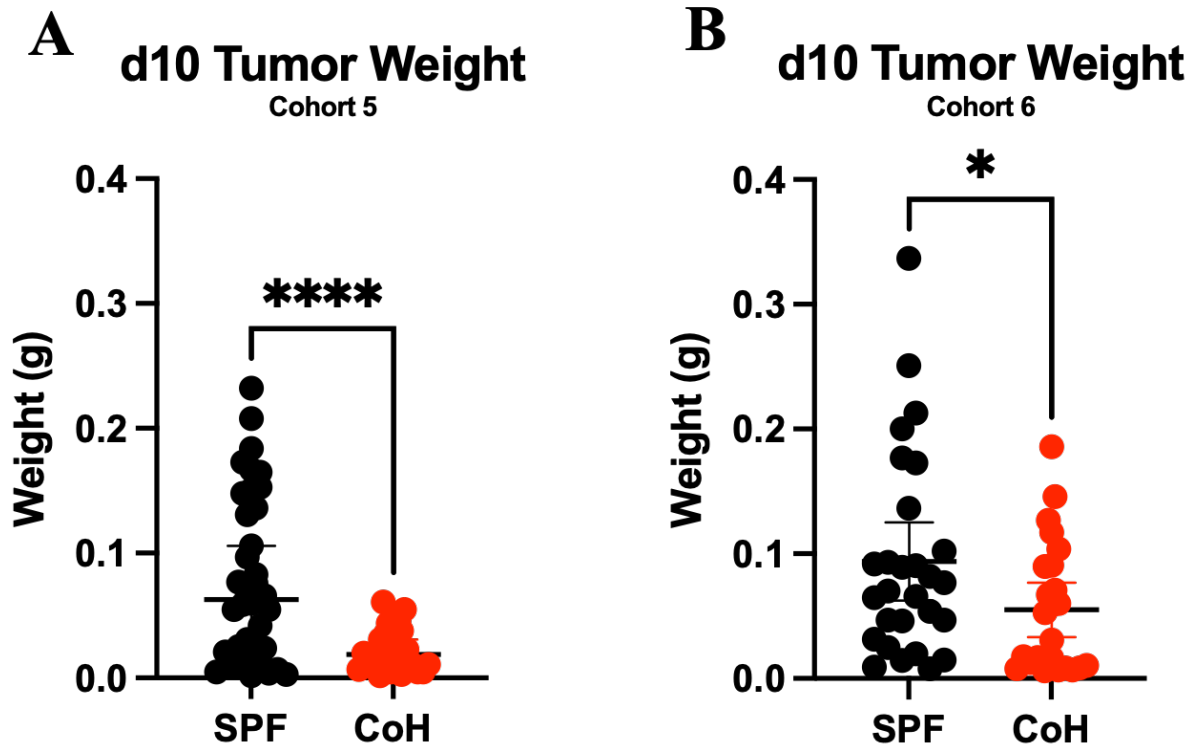
Figure 14: CoH mice have significantly smaller tumors by weight.
Subcutaneous tumors were harvested from left and right flanks of SPF and CoH mice on day 10 post-injection. Right and left tumors from each mouse were collected into separate pre-weighed 15 mL conicals of 3 mL RPMI-2% FBS and final weights were determined with a VWR 123P analytical balance. (**A**) Cohort 5 data is comprised of N = 36 SPF tumors and N = 25 CoH tumors. (**B**) Cohort 6 data is comprised of N = 28 SPF tumors and N = 24 CoH tumors. Results were repeated 2 times, as shown in this figure.

Tumor-infiltrating CD8+ T cells of CoH mice have higher PD-1 expression than SPF mice

CD8+ T cells of CoH mice are more antigen experienced, differentiated, and cytotoxic compared to SPF mice. These features of the CoH T cell repertoire may impact B16 melanoma tumor growth. To further investigate the mechanism by which CoH mice control tumor growth, we analyzed PD-1 expression by flow cytometry. PD-1 is an inhibitory receptor expressed on CD8+ T cells that can be activated by PD-L1-expressing melanoma cells. This PD-1/PD-L1 signaling inhibits CD8+ T cell effector functions, allowing melanoma cells to evade the CD8+ T cell-mediated immune response. Tissue samples were stained with antibody panel 3 (Table 1) and flow cytometry analysis was conducted. FlowJo software was used to determine the percentage of PD-1^{hi} CD8+ T cells in *ex vivo* tissue samples of both SPF and CoH mice (Figure 15).

PD-1 expression was assayed throughout the cohousing period. Upon initiation of cohousing, PD-1 expression is significantly upregulated in CoH mice by day 7 (Figure 16). Expression increases slightly by d14, and rapid downregulation occurs by d28, which results in nearly equivalent expression of PD-1 in SPF and CoH mice. This d28 observation is consistent with the results reported by Beura et al. Our timeline of PD-1 expression during cohousing is also consistent with the current understanding of PD-1 kinetics.

During a normal CD8+ T cell response, PD-1 is upregulated as a mechanism of peripheral tolerance in order to prevent autoimmunity. As previously stated, *in vivo* and *in vitro* studies have shown that PD-1 upregulation occurs rapidly during activation of naïve T cells (Yamazaki et. al, 2002; Ahn et. al, 2018). In the context of *ex vivo* blood samples, we also observe a rapid upregulated of PD-1 that peaks, on average, by day 14 in CoH mice during the cohousing period. PD-1 expression downregulates to baseline (similar to SPF mice) by day 21.

The downregulation of PD-1 between day 14 and day 21 differs from our observations of

Granzyme B (Figure 10) downregulation and contraction of LLECs (Figure 7). PD-1

downregulation occurs approximately one week prior to downregulation of Granzyme B and

contraction of LLECs during cohousing.
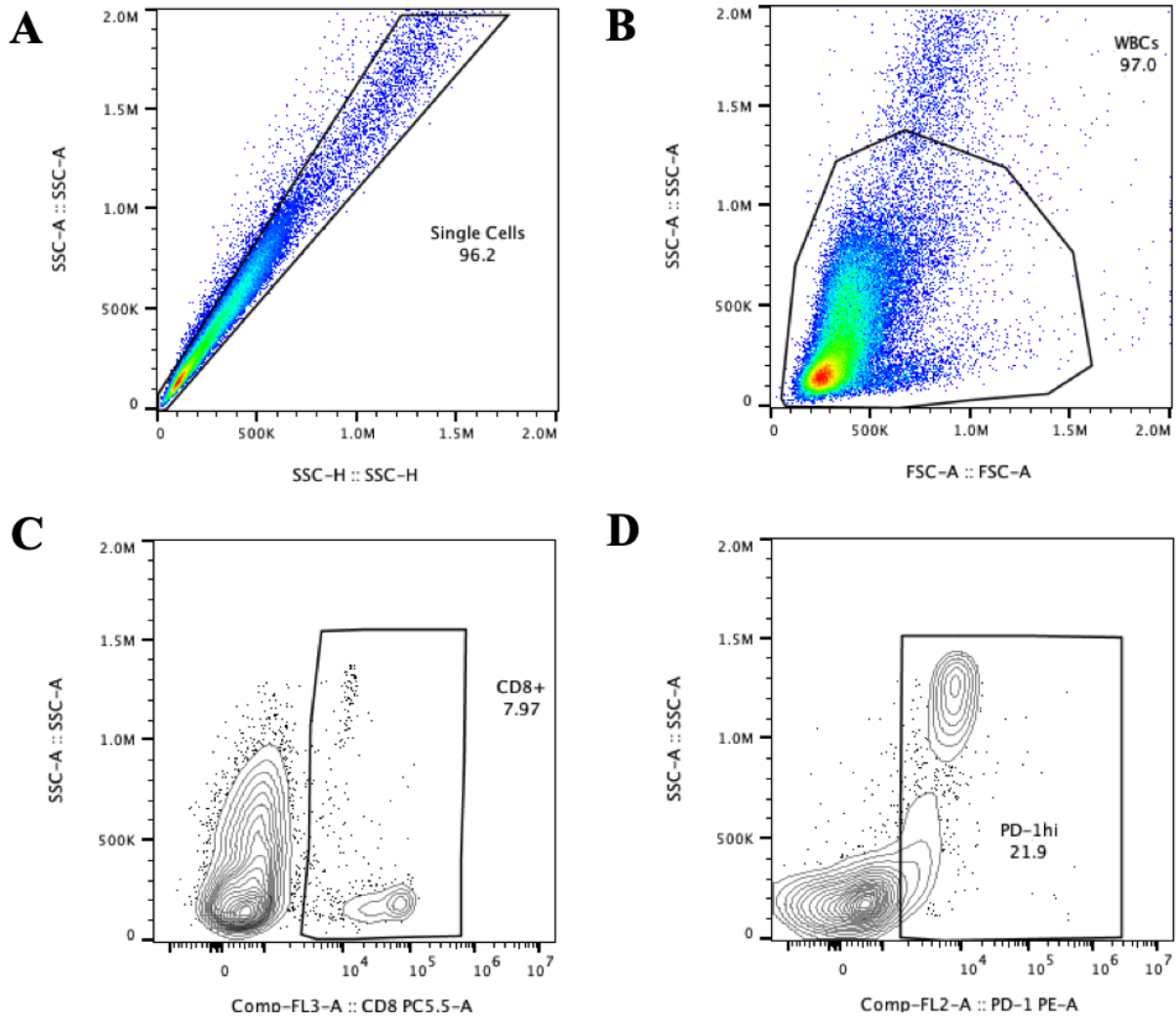
Figure 15: PD-1^{hi} CD8$^+$ gating strategy for weekly bleeds and harvest samples.
FlowJo was used to gate populations of PD-1^{hi} CD8$^+$ T cells in CoH and SPF mice from weekly bleeds and tissues from harvest. (**A**) Single cells were obtained on side-scatter height (SSC-H) by side-scatter area (SSC-A). (**B**) White blood cells (WBCs) were gated on forward-scatter area (FSC-A) by side-scatter area (SSC-A). (**C**) Distinct populations of CD8+ T cells were differentiated based on high expression of CD8 against side-scatter area (SSC-A). (**D**) Gates for PD-1^{hi} CD8$^+$ T cell populations were drawn on PD-1 by side-scatter area (SSC-A). Gating strategy was identical for all timepoints during cohousing and for all tissue harvests. Blood sample from mouse CoH 6-1 in Harvest 2 of Cohort 6 is shown above.

PD-1 expression was also assayed in the blood, spleen, dLN, and tumor at day 10 post-melanoma injection. We observed no difference in PD-1 expression between SPF and CoH mice in blood samples, though both groups experienced a twofold overall increase in PD-1^{hi} CD8+ T cell populations when compared to day 28 of cohousing (Figure 17A compared to Figure 16). This level of PD-1 expression in the blood on day 10 post-injection is similar to the level of expression observed in CoH mice between days 7 and 14 of cohousing (Figure 16).
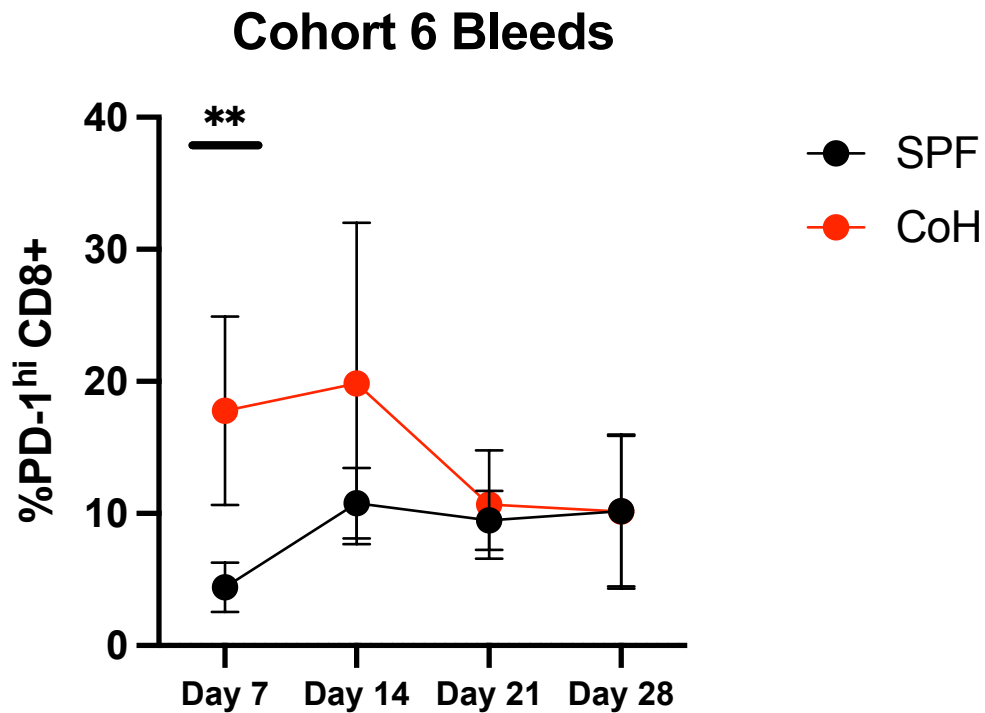
Figure 16: PD-1 is rapidly upregulated in CD8+ T cells of CoH mice during early cohousing, but expression is near equivalent in SPF and CoH mice by d28. Initial microbial exposure leads to rapid upregulation of PD-1 on CD8+ T cells of CoH mice. Downregulation occurs by day 28, where blood samples show no significant difference in PD-1 expression on CD8+ T cells of SPF and CoH mice from Cohort 6. Data points represent the mean of N = 6 mice per group. Two-way ANOVA with Bonferroni was used to determine statistical significance. Results were repeated 2 times.
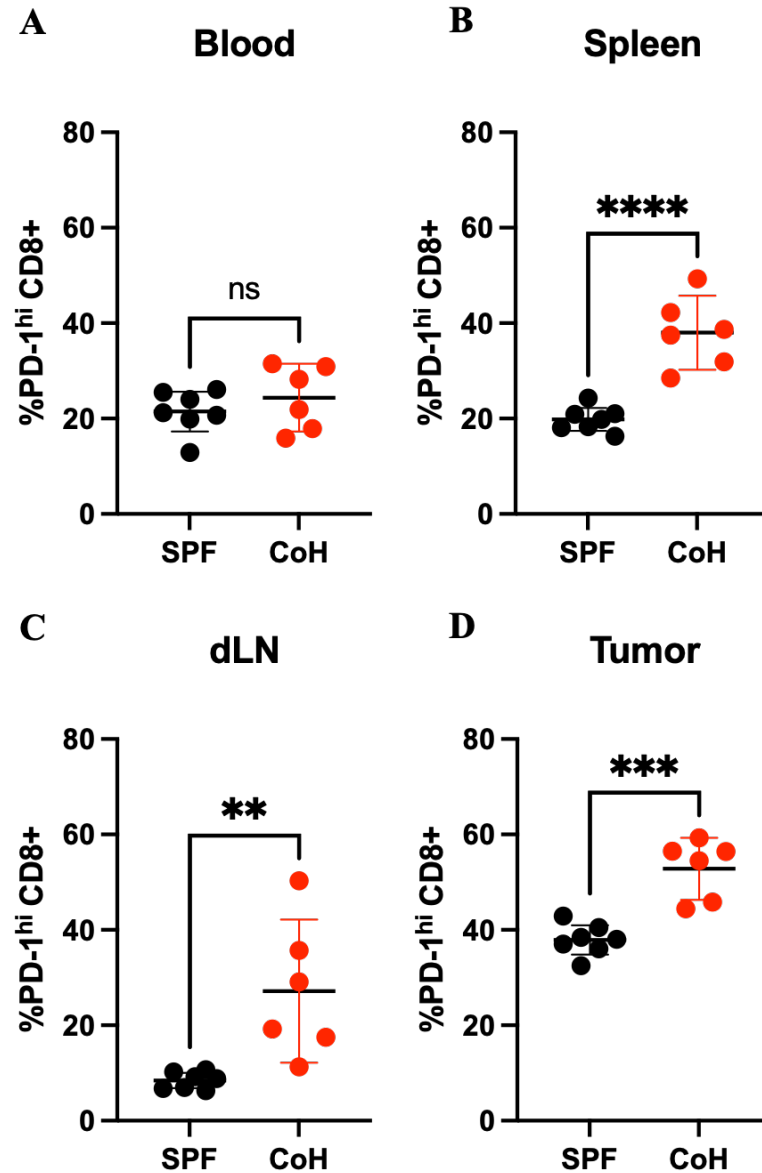
Figure 17: CoH mice have significantly increased PD-1^{hi} CD8$^+$ T cells in Spleen, dLN, and Tumor.
(**A**) No difference in PD-1 expression was observed in *ex vivo* blood samples. However, CoH mice exhibited significantly increased percentages of PD-1^{hi} CD8+ T cells in the spleen (**B**), dLN (**C**), and tumor (**D**) at d10 post-injection. Data are shown for Harvest 2 of Cohort 6 with N = 7 SPF mice and N = 6 CoH mice. Results repeated 2 times in tumor, and 3 times in all other tissues. Statistical significance was determined by unpaired t-test with all p-values < 0.05

Spleen, dLN, and tumor-infiltrating CD8+ T cells of CoH mice exhibited increased expression of PD-1. These results were repeated 3 times in blood, spleen, and dLN, while tumor results were repeated 2 times. A third repeat of tumor showed PD-1 elevation in CoH mice, but the result was not significant. Additionally, we also found that PD-1^{hi} CD8+ T cell populations in CoH mice have significantly increased gross mean fluorescence intensity (gMFI). Increased gMFI can indicate more abundant expression of the target protein (PD-1), suggesting that PD-1^{hi} cells in CoH mice express increased PD-1 per cell. Our results show that not only do CoH mice have more CD8+ T cells expressing PD-1 (Figure 17), but those PD-1-expressing cells have significantly *more* PD-1 on their surface than PD-1^{hi} CD8+ T cells of SPF mice (Figure 24, Appendix).

B16-melanoma tumor cells have increased PD-L1 expression in SPF mice

Tumor tissue samples were reduced to single cell suspension and white blood cells were separated from the melanoma tumor cells by density gradient centrifugation. Tumor cells were stained with antibody panel 6 (Table 1) and flow cytometry analysis was conducted. CD45 was used to differentiate between immune cells and non-immune cells. CD45 is a surface antigen expressed on all nucleated hematopoietic cells (Thomas & Lefrançois, 1988). By selecting for CD45- cells, we were able to rule out any PD-L1 expressing immune cells. FlowJo software was used to determine the percentage of PD-L1^{hi} tumor cells in *ex vivo* tissue samples from both SPF and CoH mice (Figure 18).

Tumor cells of SPF mice had significantly increased PD-L1 expression compared to tumor cells of CoH mice (Figure 19). Taken together with the increased PD-1 expression in

tumor-infiltrating CD8+ T cells of CoH mice (Figure 17), it appears that microbial experience

may play a role in shaping the tumor microenvironment to downregulate PD-L1 expression.
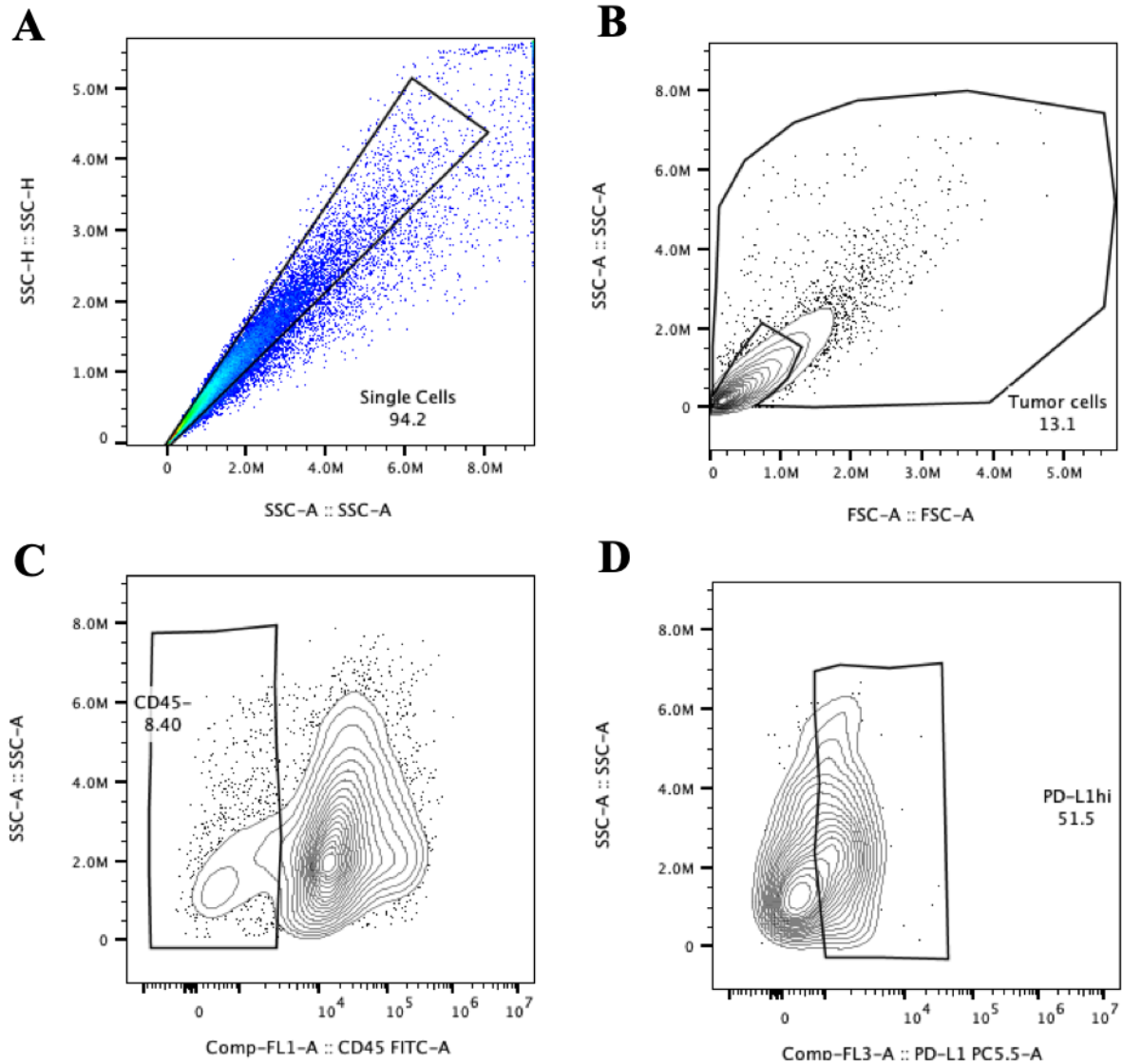
Figure 18: PD-L1^{hi} tumor cell gating strategy for harvest tumor samples.
FlowJo was used to gate populations of PD-L1^{hi} tumor cells in CoH and SPF mice from weekly bleeds and tissues from harvest. (**A**) Single cells were obtained on side-scatter area (SSC-A) by side-scatter height (SSC-H). (**B**) Tumor cells were gated on forward-scatter area (FSC-A) by side-scatter area (SSC-A) through exclusion of white blood cell region. (**C**) Distinct CD45$^-$ populations were gated on CD45 by side-scatter area (SSC-A). (**D**) Gates for PD-L1^{hi} tumor cell populations were drawn on PD-L1 by side-scatter area (SSC-A). Gating strategy was identical for all tissue harvests. Tumor pellet from mouse CoH 6-2 in Harvest 2 of Cohort 6 is shown above.

This assay was only conducted during cohort 6, as a response to the increased PD-1 expression in CoH mice coupled with their decreased tumor weights. Future experiments in the Renkema lab should aim to characterize how a microbially experienced immune system shapes development of the B16 melanoma tumor microenvironment. Beyond melanoma tumor cells, it would be helpful to explore PD-L1 expression on tumor-infiltrating cells of the innate immune system.

Figure 19: SPF mice have significantly increased PD-L1^{hi} melanoma cells.
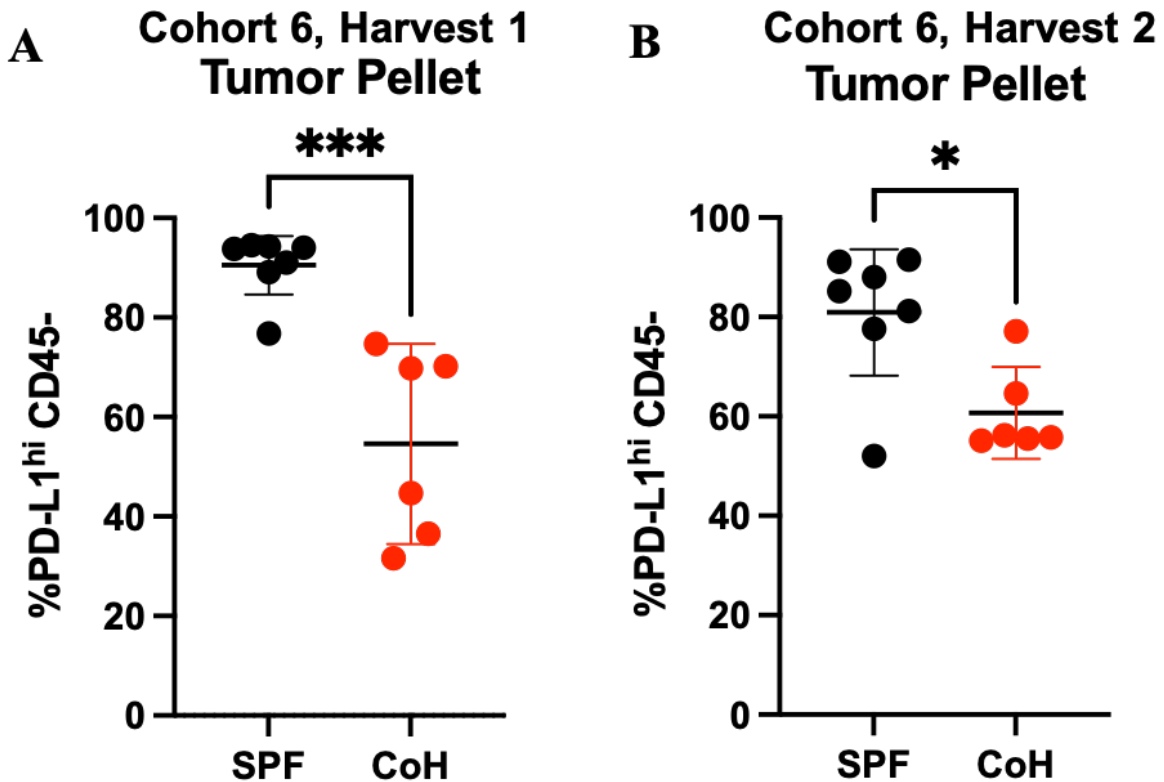Tumor cells of SPF mice show increased PD-L1 expression in samples of tumor pellet. (**A**) Data from Harvest 1 of Cohort 6 showing N = 7 SPF mice and N = 6 CoH mice. (**B**) Data from Harvest 2 of Cohort 6 showing N = 7 SPF mice and N = 6 CoH mice. Results were repeated 2 times.

Treatment with anti-PD-1 during *in vitro* stimulation may increase cytotoxicity of CD8⁺ T cells in CoH mice

We have shown that, compared to SPF mice, tumor-infiltrating CD8+ T cells of CoH mice are more cytotoxic, have increased PD-1 expression, and are found in tumors with lower PD-L1 expression. To further investigate how PD-1/PD-L1 interactions within the tumor microenvironment impact CD8+ T cell cytotoxicity, we conducted an *in vitro* checkpoint blockade assay.

Tumor-infiltrating CD8+ T cells from both SPF and CoH mice were cultured and stimulated with anti-CD3, anti-CD28, and supported with IL-2. Analogous tumor cells were added to each experimental well (not added to control wells). These conditions were designed to recreate the tumor microenvironment *in vitro*. Anti-PD-1 and/or anti-CTLA-4 antibodies were added to the experimental wells and incubated for 3 days. 1 mL of supernatant was collected from each well and frozen for future analysis. Remaining cell suspensions were stained with antibody panels 1-2 (Table 1) and flow cytometry analysis was conducted. FlowJo software was used to determine the percentage of GzB^{hi} CD8+ T cells in SPF and CoH mice 3 days after *in vitro* stimulation. A consistent gating strategy was applied to all *in vitro* stimulation data (Figure 12).

Consistent with our results reported in Figure 13, we show that CoH mice exhibit an increased proportion of GzB^{hi} CD8+ T cells 3 days after *in vitro* stimulation under control conditions (Figure 20). In the presence of analogous tumor cells (+Tumor), it appears that overall cytotoxicity is diminished in both SPF and CoH mice compared to control, presumably due to the addition of PD-L1 expressing tumor cells. CoH mice retain higher proportions of cytotoxic CD8+ T cells after addition of analogous B16 melanoma tumor cells, though the difference is not significant. When anti-PD-1 treatment is added, we observe a very slight increase in GzB^{hi} CD8+

T cells in CoH mice compared to the +Tumor condition. The same result is observed for anti-PD-1/anti-CTLA-4 combination therapy. Conversely, SPF mice show a slight decrease in GzB^{hi} CD8+ T cells after anti-PD-1 and anti-PD-1/anti-CTLA-4 treatment compared to the +Tumor condition.
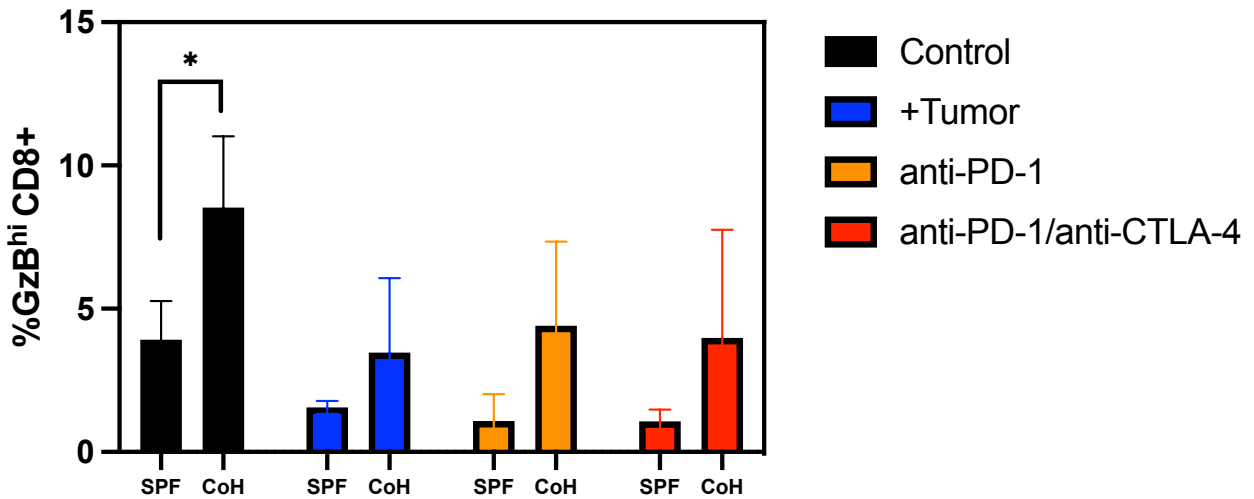
Figure 20: Treatment with anti-PD-1 marginally increases GzB^{hi} CD8^{+} T cell populations in CoH mice after *in vitro* stimulation.
Tumor-infiltrating CD8+ T cells of CoH mice have significantly higher expression of Granzyme B after *in vitro* stimulation. Addition of analogous tumor cells results in an overall decrease in GzB^{hi} CD8+ T cell populations, while addition of anti-PD-1 or combination anti-PD-1/anti-CTLA-4 therapy resulted in marginal increases in GzB^{hi} CD8+ T cell populations in CoH mice. All groups represent N = 3 mice. Statistical significance was determined by individual unpaired t test per condition and Two-way ANOVA with Tukey's returned no significance. Results have not been repeated.

CHAPTER 5: DISCUSSION

To our knowledge, we are the only lab conducting cancer research in a cohoused mouse model. For reasons presented in this thesis, the use of cohoused mice in immunology research complements studies typically conducted with SPF mice. Not only do our results showcase the value of microbial experience in bolstering anti-tumor immunity, but they also highlight the potential deficiencies of research conducted solely in SPF mice. Here, we have used multiple modalities to show that microbial experience improves the anti-tumor immune response of CoH mice compared to SPF mice.

CoH mice were generated by cohousing SPF mice with PS mice for 28 days. Transfer of common murine pathogens was confirmed by Charles River Research Animal Diagnostic Services (CR-RADS). Throughout the cohousing period, we observed increasing populations of $CD44^{hi}KLRG1^{hi}$ CD8+ T cells in CoH mice, while these populations remained nearly absent in SPF mice. This phenotype indicated upregulation of CD44 in response to antigen exposure, as well as upregulation of KLRG1, which indicates differentiation of long-lived effector cells (LLECs). These CD8+ T cell populations display characteristics of both long-term memory pools as well as short-term effectors (Renkema et. al, 2020), and our results suggest that microbial exposures act to increase the presence LLECs in CoH mice after 28 days of cohousing.

While this population of LLECs is typically quite small, they have been shown to display robust cytotoxicity (Renkema et. al, 2020). As such, $CD44^{hi}KLRG1^{hi}$ remains a phenotype of interest due to its potential application in CD8+ T cell-mediated cancer vaccination strategies. Our results are consistent with data collected from previous cohorts in the Renkema lab (Groeber, 2020).

We then investigated the role of CD44^{hi}KLRG1^{hi} CD8+ T cells in response to B16 melanoma challenge. At day 10 post-melanoma injection, we saw that CoH mice further increased expression of CD44^{hi}KLRG1^{hi} CD8+ T cells in the blood compared to day 28 of cohousing. This indicates the potential for further expansion of this antigen-experienced, differentiated, LLEC phenotype when challenged by B16 melanoma. This increase in CD44^{hi}KLRG1^{hi} CD8+ T cell populations was also observed in tissue samples from the spleen, dLN, and tumor of CoH mice. Notably, this phenotype is largely absent in the blood, spleen, and dLN of SPF mice, though its presence in the tumor is significant.

Previous studies have shown that LLECs (CD44^{hi}KLRG1^{hi} phenotype) are found in decreasing proportions in the blood, spleen, and dLN, respectively (Olson et. al, 2013). Our results confirm the findings of Olson et al, while adding that LLECs are capable of infiltrating the tumor microenvironment. In fact, our results indicate that the CD44^{hi}KLRG1^{hi} phenotype comprises the majority of tumor-infiltrating CD8+ T cells in both SPF and CoH mice, though this proportion is significantly higher in CoH mice. Further investigation is needed to better characterize this tumor preference of LLECs in SPF mice.

It is clear that challenge with B16 melanoma elicits an immune response from both SPF and CoH mice, but CoH mice possess greater populations of antigen experienced, differentiated CD8+ T cells. Further experiments were conducted to determine the cytotoxicity of these populations and their role in anti-tumor immunity.

Microbial experience induces more antigen experienced and differentiated CD8+ T cell populations in CoH mice, which led us to further investigate their cytotoxic capacity. We measured cytotoxicity by expression of Granzyme B throughout cohousing and at 10 days post-melanoma injection. We observed significantly increased GzB^{hi} CD8+ T cell populations in CoH

mice by day 14 of cohousing, followed by a period of GzB downregulation that is consistent with the contraction phase of immunity. These results confirmed previous findings from the Renkema lab showing that GzB expression peaks early in the cohousing period, and is downregulated over time. However, our results differed slightly from those previously reported, as GzB expression peaked on day 14 in our cohorts, while prior cohorts showed GzB expression peaking by day 7 (Groeber, 2020). This difference is likely caused by variations in pathogen transfer from PS to CoH mice.

Additionally, our trend of GzB expression over time coincided with our observations of CD44^{hi}KLRG1^{hi} expression over time, suggesting that these may be the same T cell populations. To better understand this relationship, GzB^{hi}KLRG1^{hi} CD8+ T cells were observed over time, and we found that this phenotype was almost identical in proportion and trend to the GzB^{hi} CD8+ T cell populations (Figure 23, Appendix). This result is noteworthy as it again indicates an LLEC phenotype in its retention of KLRG1 expression after contraction (Renkema et. al, 2020). An upgrade to our flow cytometer's license would permit us to stain with more antibodies per panel. This would make it possible to more accurately and efficiently investigate the presence of LLEC phenotypes such as CD44^{hi}KLRG1^{hi}GzB^{hi} CD8+ T cells. For now, these comparisons provide some evidence that our CD44^{hi}KLRG1^{hi} populations and GzB^{hi} populations are one and the same.

GzB expression remained elevated in CoH mice at 10 days post-melanoma injection. This trend was observed in *ex vivo* tissue samples of blood, spleen, dLN, and tumor. The proportion of GzB^{hi} tumor-infiltrating CD8+ T cells in CoH mice was nearly twofold greater than the proportion observed in SPF mice. These findings were again confirmed in cell culture

after *in vitro* stimulation, showing that GzB[hi] tumor-infiltrating CD8+ T cells of CoH mice are inherently more cytotoxic than cells from SPF mice.

Taken together, these results indicate that previous microbial exposure may prime CD8+ T cells to mount a more robust cytotoxic intratumoral immune response. Further experiments should be conducted to examine the anti-tumor potential of CD8+ T cells adoptively transferred from CoH mice.

To this point, we have established that CD8+ T cells of CoH mice are more antigen-experienced, differentiated, and cytotoxic after 28 days of cohousing, as well as 10 days post-melanoma injection. These findings have all been confirmed and repeated 2-3 times, and differences in cytotoxicity have been shown *in vitro* as well. We then investigated whether or not this increase in cytotoxicity would translate to increased control of tumor growth in CoH mice.

Previous studies have shown the importance of the microbiome in controlling tumor growth. One study reconstituted the gut microbiome of SPF mice through oral gavage of ileocecal material from wild mice. They showed that colorectal tumor growth was better controlled in SPF mice with a reconstituted gut microbiome compared to standard SPF mice (Rosshart et. al, 2017). Another study showed that cancer treatments were more effective at controlling tumor growth in mice with a healthy gut microbiota (Iida et. al, 2013). Our results are consistent with these findings. In two cohorts of mice, we've shown that mice with microbial experience (CoH) have significantly smaller tumors than mice with no microbial experience (SPF). These results suggest that microbial experience may provide protection against tumor growth.

An attempt was made to compare the rate of tumor growth in SPF and CoH mice. We tried to gather tumor area data by collecting daily tumor measurements with a digital caliper.

Unfortunately, these measurements were inconsistent and difficult to collect due to nature of B16 melanoma tumor growth. The tumors remain quite small until approximately day 7 or 8 post-injection, at which point, their size drastically increases. To collect these measurements in future cohorts, the timepoint for harvest may need to be extended beyond day 10 post-injection. This change would serve two purposes. First, it would allow us to take more accurate measurements of late-stage tumor growth, as the tumors would be larger. Secondly, it would help us determine the longevity of the tumor growth-control observed in CoH mice.

PD-1 is relevant biomarker in the context of anti-tumor immunity, largely due to its inhibitory function on effector CD8+ T cells. The significant differences in tumor weight observed between SPF and CoH mice suggested the possibility that CD8+ T cells of CoH mice have decreased expression of PD-1. If so, decreased PD-1 expression may function to preserve anti-tumor immunity by allowing CD8+ T cells to retain their effector function and ability to lyse cancerous cells, thus resulting in decreased tumor burden. My hypothesis was quickly proven wrong when analyzing *ex vivo* tissue data from day 10 post-melanoma injection. CoH mice have significantly increased PD-1 expression in the spleen, dLN, and tumor. However, there is effectively no difference in PD-1 expression in the blood. Furthermore, gMFI analysis indicated that PD-1-expressing cells of CoH mice have significantly more PD-1 on their surface than PD-1^{hi} CD8+ T cells of SPF mice.

During a normal activated CD8+ T cell response, PD-1 is upregulated as a mechanism of peripheral tolerance in order to prevent autoimmunity. We have shown that microbial exposure leads to increased activation of CD8+ T cells and increased upregulation of PD-1 in CD8+ T cells of CoH mice during cohousing. Downregulation of PD-1 precedes downregulation of GzB and LLEC contraction by approximately 7 days during cohousing. Future experiments should try

to determine if the observed populations of LLECs and PD-1^{hi} CD8+ T cells are one and the same.

We've shown that CD8+ T cells of CoH mice are more antigen experienced, differentiated, cytotoxic, and they control tumor growth better than SPF mice. However, they also exhibit increased expression of PD-1, which could increase susceptibility to effector function inhibition by PD-L1 expressing melanoma cells. After observing preliminary data from cohort 5, we decided to investigate differences in PD-L1 expression within the tumor microenvironment.

Tumor cells of SPF mice had significantly increased PD-L1 expression compared to tumor cells of CoH mice. This result suggests that microbial experience may play a role in shaping the tumor microenvironment to downregulate PD-L1 expression. Future experiments should be done to characterize PD-L1 expression in the tumor microenvironment of CoH and SPF mice. It has been shown that IFN-γ is one of the most potent inducers of PD-L1 expression (Zhang & Wang, 2019). Supernatant from tumor sample cell cultures was collected and stored for future ELISA analysis. Results of those assays may provide insight into why PD-L1 expression is elevated in SPF mice.

To further examine how PD-1/PD-L1 interactions are impacted by microbial experience, we developed a novel *in vitro* checkpoint blockade assay. Tumor samples were processed into single cell suspension and white blood cells were purified by density gradient centrifugation. Tumor-infiltrating white blood cells were stimulated in culture with anti-CD3/anti-CD28 and IL-2. Analogous tumor cells were added to the culture, as well as anti-PD-1 and/or anti-CTLA-4 for the experimental conditions.

CoH mice exhibit an increased proportion of GzB^{hi} CD8+ T cells under control conditions, and overall cytotoxicity is diminished in the +Tumor condition for both SPF and CoH mice compared to control. This result seemed reasonable considering the addition of PD-L1 expressing tumor cells. The remaining comparisons in this assay yielded no significant results, but provided trends that may inform future experiments. We see that CoH mice retain higher proportions of cytotoxic CD8+ T cells after challenge with B16 melanoma tumor cells, and when anti-PD-1 treatment is added, we observe a very slight increase in GzB^{hi} CD8+ T cells compared to the +Tumor condition. The same result is observed for anti-PD-1/anti-CTLA-4 combination therapy. However, SPF mice show a slight decrease in GzB^{hi} CD8+ T cells after anti-PD-1 and anti-PD-1/anti-CTLA-4 treatment compared to the +Tumor condition.

While the control group provided the only significant result between SPF and CoH mice, the trends observed in the treatment groups justify further investigation. Our *in vitro* checkpoint blockade assay is novel, and the protocol will undoubtedly require further fine-tuning. Future *in vitro* checkpoint blockade experiments in the Renkema lab should aim to increase tumor-infiltrating CD8+ T cell counts through additional density gradient centrifugation or increased "mini-pooling" of samples from multiple mice. Additional experimentation to determine effective doses of anti-PD-1 and/or anti-CTLA-4 would also be beneficial.

It is possible that SPF mice remain refractory to anti-PD-1 therapy due to their decreased PD-1 expressing CD8+ T cells and increased PD-L1 expression on melanoma tumor cells within the SPF tumor microenvironment. Conversely, CoH mice may be more responsive to anti-PD-1 therapy due to microbial exposure that resulted in increased PD-1 expressing CD8+ T cell populations and decreased PD-L1 expression in the CoH tumor microenvironment.

This thesis shows that CoH mice exhibit significantly increased populations of antigen experienced, differentiated, and cytotoxic CD8+ T cells in blood, spleen, tumor-draining lymph nodes, and tumor. CD8+ T cells of CoH mice also exhibit significantly increased PD-1 expression and slight increases in the efficacy of *in vitro* anti-PD-1 immunotherapy. Most importantly, our data show that CoH mice have superior anti-tumor immunity as evidenced by their significantly lower tumor weights when compared to the larger tumors of SPF mice. Taken together, our results show that microbial experience increases cytotoxicity of tumor-infiltrating CD8+ T cells and controls tumor growth.
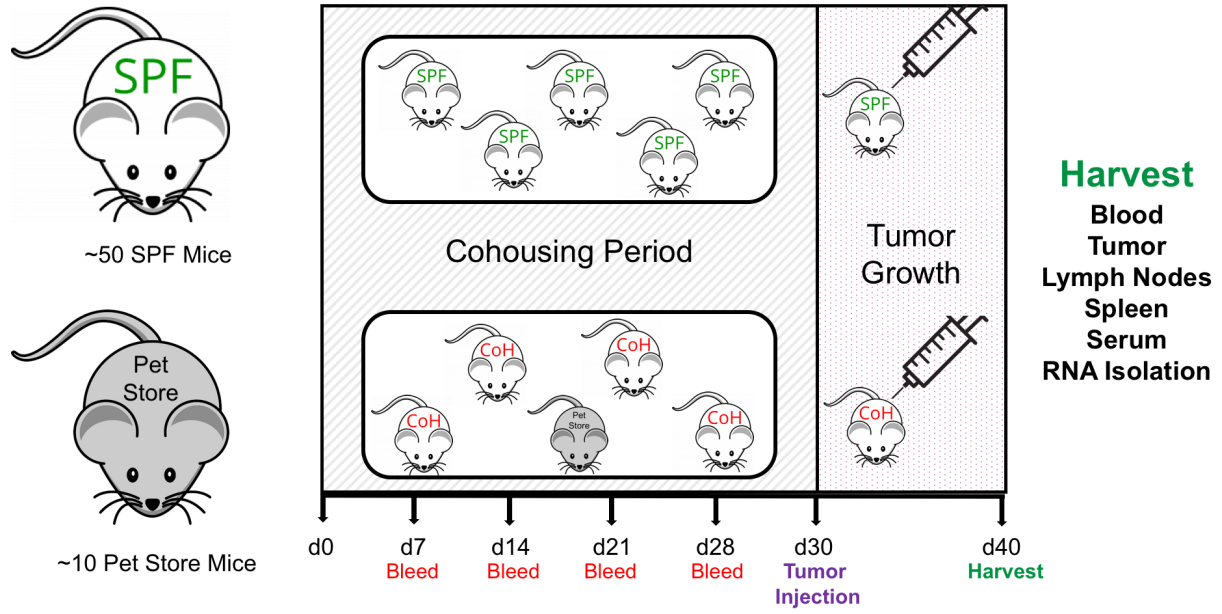
Figure 21: Experimental design for producing cohoused mice.

SPF Tumor   **CoH Tumor**

Figure 22: Comparison of SPF vs. CoH tumor sizes and blood supply.
While these images lack an appropriate measurement for scale, they do provide a good
visual example of the tumor-associated angiogenesis consistently observed in SPF mice.

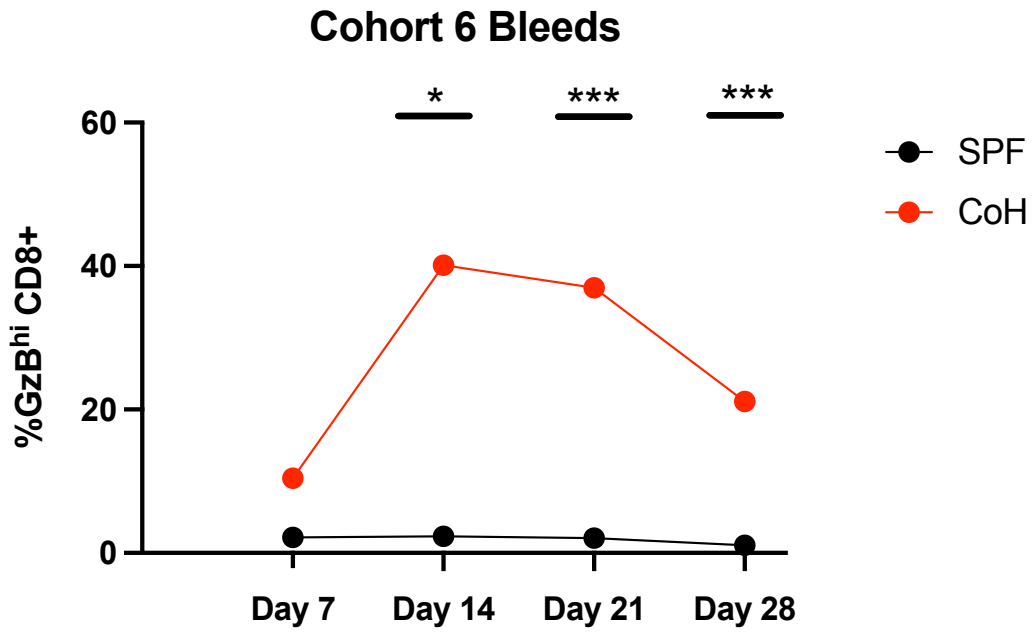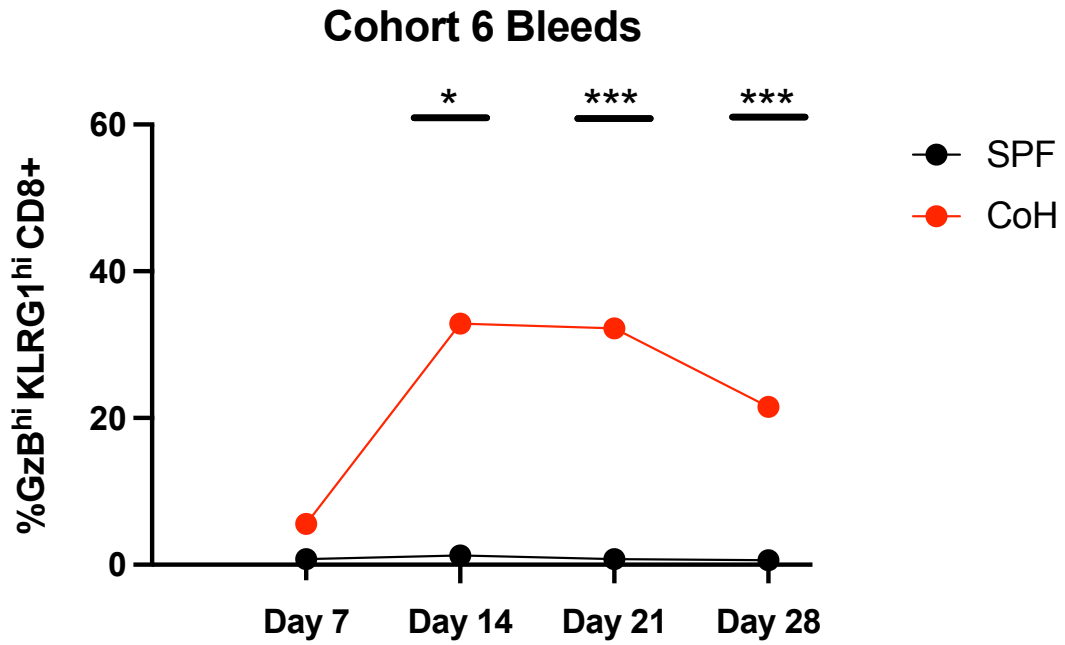**Figure 23: GzB^{hi}KLRG1^{hi} CD8+ T cells are elevated in CoH mice during cohousing period of 28 days, and are nearly identical in proportion and trend to GzB^{hi} CD8+ T cells.**

A **Blood**

B **Spleen**
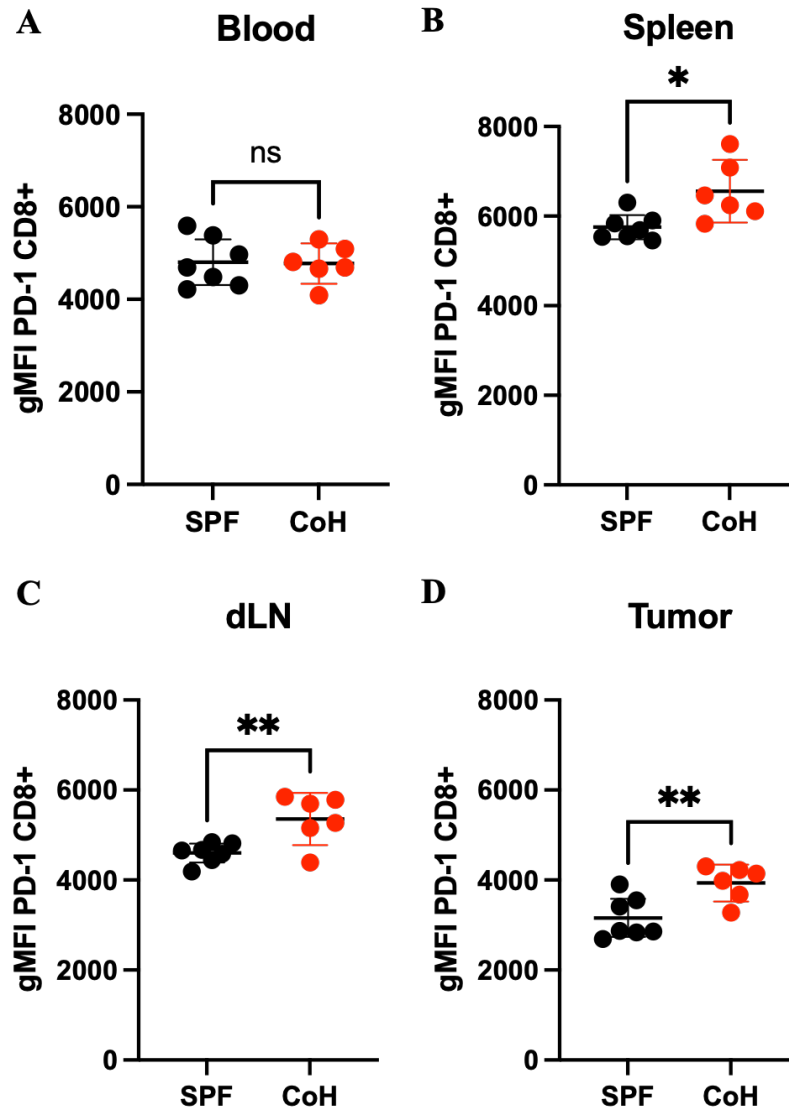
C **dLN**

D **Tumor**

Figure 24: PD-1^{hi} CD8+ T cell populations in CoH mice have significantly increased gross mean fluorescence intensity (gMFI) compared to SPF mice.

REFERENCES

Abolins, Stephen, Elizabeth C. King, Luke Lazarou, Laura Weldon, Louise Hughes, Paul Drescher, John G. Raynes, Julius C. R. Hafalla, Mark E. Viney, and Eleanor M. Riley. "The Comparative Immunology of Wild and Laboratory Mice, Mus Musculus Domesticus." *Nature Communications* 8, no. 1 (August 2017): 14811. https://doi.org/10.1038/ncomms14811.

Ahn, Eunseon, Koichi Araki, Masao Hashimoto, Weiyan Li, James L. Riley, Jeanne Cheung, Arlene H. Sharpe, Gordon J. Freeman, Bryan A. Irving, and Rafi Ahmed. "Role of PD-1 during Effector CD8 T Cell Differentiation." Proceedings of the National Academy of Sciences of the United States of America 115, no. 18 (May 1, 2018): 4749–54. https://doi.org/10.1073/pnas.1718217115.

Andersen, Mads Hald, David Schrama, Per thor Straten, and Jürgen C. Becker. "Cytotoxic T Cells." *Journal of Investigative Dermatology* 126, no. 1 (January 2006): 32–41. https://doi.org/10.1038/sj.jid.5700001.

Baaten, Bas JG, Cheng-Rui Li, and Linda M Bradley. "Multifaceted Regulation of T Cells by CD44." *Communicative & Integrative Biology* 3, no. 6 (2010): 508–12. https://doi.org/10.4161/cib.3.6.13495.

Beura, Lalit K., Sara E. Hamilton, Kevin Bi, Jason M. Schenkel, Oludare A. Odumade, Kerry A. Casey, Emily A. Thompson, et al. "Normalizing the Environment Recapitulates Adult Human Immune Traits in Laboratory Mice." *Nature* 532, no. 7600 (April 2016): 512–16. https://doi.org/10.1038/nature17655.

Blank, Christian, Ian Brown, Amy C. Peterson, Mike Spiotto, Yoshiko Iwai, Tasuku Honjo, and Thomas F. Gajewski. "PD-L1/B7H-1 Inhibits the Effector Phase of Tumor Rejection by T Cell Receptor (TCR) Transgenic CD8+ T Cells." *Cancer Research* 64, no. 3 (February 1, 2004): 1140–45. https://doi.org/10.1158/0008-5472.CAN-03-3259.

Cicin-Sain, Luka, James D. Brien, Jennifer L. Uhrlaub, Anja Drabig, Thomas F. Marandu, and Janko Nikolich-Zugich. "Cytomegalovirus Infection Impairs Immune Responses and Accentuates T-Cell Pool Changes Observed in Mice with Aging." Edited by Karen L. Mossman. *PLoS Pathogens* 8, no. 8 (August 16, 2012): e1002849. https://doi.org/10.1371/journal.ppat.1002849.

Curtsinger, Julie M., Michael Y. Gerner, Debra C. Lins, and Matthew F. Mescher. "Signal 3 Availability Limits the CD8 T Cell Response to a Solid Tumor." *The Journal of Immunology* 178, no. 11 (June 1, 2007): 6752–60. https://doi.org/10.4049/jimmunol.178.11.6752.

DiSpirito, Joanna R, and Hao Shen. "Quick to Remember, Slow to Forget: Rapid Recall Responses of Memory CD8+ T Cells." Cell Research 20, no. 1 (January 2010): 13–23. https://doi.org/10.1038/cr.2009.140.

Dou, Jun, Meng Pan, Ping Wen, Yating Li, Quan Tang, Lili Chu, Fengshu Zhao, et al. "Isolation and Identification of Cancer Stem Like Cells From Murine Melanoma Cell Lines." *Cellular & Molecular Immunology* 4 (January 1, 2008): 467–72.

El Jamal, Siraj, Abdulhadi Alamodi, Renate Wahl, Zakaria Grada, Mohammad Shareef, Sofie Hassan, Fadi Murad, et al. "Melanoma Stem Cell Maintenance and Chemo-Resistance Are Mediated by CD133 Signal to PI3K-Dependent Pathways." *Oncogene* 39 (August 6, 2020). https://doi.org/10.1038/s41388-020-1373-6.

Garcia-Diaz, Angel, Daniel Sanghoon Shin, Blanca Homet Moreno, Justin Saco, Helena Escuin-Ordinas, Gabriel Abril Rodriguez, Jesse M. Zaretsky, et al. "Interferon Receptor Signaling Pathways Regulating PD-L1 and PD-L2 Expression." *Cell Reports* 19, no. 6 (May 9, 2017): 1189–1201. https://doi.org/10.1016/j.celrep.2017.04.031.

Gerdes, J., H. Lemke, H. Baisch, H. H. Wacker, U. Schwab, and H. Stein. "Cell Cycle Analysis of a Cell Proliferation-Associated Human Nuclear Antigen Defined by the Monoclonal Antibody Ki-67." *Journal of Immunology* (Baltimore, Md.: 1950) 133, no. 4 (October 1984): 1710–15.

Griffin M.E., Espinosa J., Becker J.L., Luo J.D., Carroll T.S., Jha J.K., Fanger G.R., Hang H.C. "Enterococcus peptidoglycan remodeling promotes checkpoint inhibitor cancer immunotherapy." *Science*. 2021 Aug 27;373(6558):1040-1046. doi: 10.1126/science.abc9113. PMID: 34446607.

Groeber, Hanna. 2020. "Microbial Experience Influences Tumor- Infiltrating T Lymphocytes." Grand Valley State University. https://scholarworks.gvsu.edu/theses/991.

Hamid, O, C Robert, A Daud, F S Hodi, W J Hwu, R Kefford, J D Wolchok, et al. "Five-Year Survival Outcomes for Patients with Advanced Melanoma Treated with Pembrolizumab in KEYNOTE-001." Annals of Oncology 30, no. 4 (April 2019): 582–88. https://doi.org/10.1093/annonc/mdz011.

Hanahan, Douglas. "Hallmarks of Cancer: New Dimensions." *Cancer Discovery* 12, no. 1 (January 2022): 31–46. https://doi.org/10.1158/2159-8290.CD-21-1059.

Hanahan, Douglas, and Robert A. Weinberg. "Hallmarks of Cancer: The Next Generation." *Cell* 144, no. 5 (March 2011): 646–74. https://doi.org/10.1016/j.cell.2011.02.013.

Huggins, Mathew A., Stephen C. Jameson, and Sara E. Hamilton. "Embracing Microbial Exposure in Mouse Research." *Journal of Leukocyte Biology* 105, no. 1 (January 2019): 73–79. https://doi.org/10.1002/JLB.4RI0718-273R.

Iida, Noriho, Amiran Dzutsev, C. Andrew Stewart, Loretta Smith, Nicolas Bouladoux, Rebecca A. Weingarten, Daniel A. Molina, et al. "Commensal Bacteria Control Cancer Response to Therapy by Modulating the Tumor Microenvironment." Science

(New York, N.Y.) 342, no. 6161 (November 22, 2013): 967–70.
https://doi.org/10.1126/science.1240527.

Jin, Chengcheng, Georgia Lagoudas, Chen Zhao, Susan Bullman, Arjun Bhutkar, Bo Hu, Samuel
Ameh, et al. "Commensal Microbiota Promote Lung Cancer Development via Γδ T Cells."
Cell 176, no. 5 (February 21, 2019): 998-1013.e16.
https://doi.org/10.1016/j.cell.2018.12.040.

Keir, Mary E., Spencer C. Liang, Indira Guleria, Yvette E. Latchman, Andi Qipo, Lee A.
Albacker, Maria Koulmanda, Gordon J. Freeman, Mohamed H. Sayegh, and Arlene H.
Sharpe. "Tissue Expression of PD-L1 Mediates Peripheral T Cell Tolerance." *The Journal
of Experimental Medicine* 203, no. 4 (April 17, 2006): 883–95.
https://doi.org/10.1084/jem.20051776.

Kloskowski, Tomasz, Joanna Jarząbkowska, Arkadiusz Jundziłł, Daria Balcerczyk,
Monika Buhl, Kamil Szeliski, Magdalena Bodnar, et al. "CD133 Antigen as a
Potential Marker of Melanoma Stem Cells: In Vitro and In Vivo Studies." Edited by
Mustapha Najimi. *Stem Cells International* 2020 (December 23, 2020): 1–10.
https://doi.org/10.1155/2020/8810476.

Leach, Dana R., Krummel, Matthew F., and Allison, James P. "Enhancement of
Antitumor Immunity by CTLA-4 Blockade." *Science* 271, no. 5256 (March 22,
1996): 1734–36.

Masopust, David, and Jason M. Schenkel. "The Integration of T Cell Migration, Differentiation
and Function." *Nature Reviews Immunology* 13, no. 5 (May 2013): 309–20.
https://doi.org/10.1038/nri3442.

Masopust, David, Christine P. Sivula, and Stephen C. Jameson. "Of Mice, Dirty Mice, and Men:
Using Mice To Understand Human Immunology." *The Journal of Immunology* 199, no. 2
(July 15, 2017): 383–88. https://doi.org/10.4049/jimmunol.1700453.

Marshall, Jean S., Richard Warrington, Wade Watson, and Harold L. Kim. "An Introduction to
Immunology and Immunopathology." Allergy, Asthma, and Clinical Immunology: *Official
Journal of the Canadian Society of Allergy and Clinical Immunology* 14, no. Suppl 2
(September 12, 2018): 49. https://doi.org/10.1186/s13223-018-0278-1.

McLane, Laura M., Mohamed S. Abdel-Hakeem, and E. John Wherry. "CD8 T Cell Exhaustion
During Chronic Viral Infection and Cancer." *Annual Review of Immunology* 37, no. 1
(2019): 457–95. https://doi.org/10.1146/annurev-immunol-041015-055318.

Mescher, Matthew F., Julie M. Curtsinger, Pujya Agarwal, Kerry A. Casey, Michael Gerner,
Christopher D. Hammerbeck, Flavia Popescu, and Zhengguo Xiao. "Signals Required for
Programming Effector and Memory Development by CD8+ T Cells." *Immunological
Reviews* 211, no. 1 (2006): 81–92. https://doi.org/10.1111/j.0105-2896.2006.00382.x.

Miller, Peter L., and Tiffany L. Carson. "Mechanisms and Microbial Influences on CTLA-4 and PD-1-Based Immunotherapy in the Treatment of Cancer: A Narrative Review." *Gut Pathogens* 12, no. 1 (December 2020): 43. https://doi.org/10.1186/s13099-020-00381-6.

Morse III, H. "Building a Better Mouse: One Hundred Years of Genetics and Biology." In The Mouse in Biomedical Research, I:1–11. Elsevier, 2007. https://doi.org/10.1016/B978-012369454-6/50013-3.

Nishimura H, Okazaki T, Tanaka Y, Nakatani K, Hara M, Matsumori A, Sasayama S, Mizoguchi A, Hiai H, Minato N, Honjo T. Autoimmune dilated cardiomyopathy in PD-1 receptor-deficient mice. *Science*. 2001 Jan 12;291(5502):319-22. doi: 10.1126/science.291.5502.319. PMID: 11209085.

Nowacki, Tobias M., Stefanie Kuerten, Wenji Zhang, Carey L. Shive, Christian R. Kreher, Bernhard O. Boehm, Paul V. Lehmann, and Magdalena Tary-Lehmann. "Granzyme B Production Distinguishes Recently Activated CD8+ Memory Cells from Resting Memory Cells." *Cellular Immunology* 247, no. 1 (May 2007): 36–48. https://doi.org/10.1016/j.cellimm.2007.07.004.

Olson, Janelle A., Cameron McDonald-Hyman, Stephen C. Jameson, and Sara E. Hamilton. "Effector-like CD8+ T Cells in the Memory Population Mediate Potent Protective Immunity." *Immunity* 38, no. 6 (June 27, 2013): 1250–60. https://doi.org/10.1016/j.immuni.2013.05.009.

Overwijk, Willem W., and Nicholas P. Restifo. "B16 as a Mouse Model for Human Melanoma." *Current Protocols in Immunology* / Edited by John E. Coligan ... [et Al.] CHAPTER (May 2001): Unit-20.1. https://doi.org/10.1002/0471142735.im2001s39.

Phan, Giao Q., James C. Yang, Richard M. Sherry, Patrick Hwu, Suzanne L. Topalian, Douglas J. Schwartzentruber, Nicholas P. Restifo, et al. "Cancer Regression and Autoimmunity Induced by Cytotoxic T Lymphocyte-Associated Antigen 4 Blockade in Patients with Metastatic Melanoma." *Proceedings of the National Academy of Sciences of the United States of America* 100, no. 14 (July 8, 2003): 8372–77. https://doi.org/10.1073/pnas.1533209100.

Padmanee Sharma and James P. Allison. "The Future of Immune Checkpoint Therapy." *Science* 348, no. 6230 (April 3, 2015): 56–61.

Pushalkar, Smruti, Mautin Hundeyin, Donnele Daley, Constantinos P. Zambirinis, Emma Kurz, Ankita Mishra, Navyatha Mohan, et al. "The Pancreatic Cancer Microbiome Promotes Oncogenesis by Induction of Innate and Adaptive Immune Suppression." *Cancer Discovery* 8, no. 4 (April 2018): 403–16. https://doi.org/10.1158/2159-8290.CD-17-1134.

Qin, Shuyang S., Booyeon J. Han, Alyssa Williams, Katherine M. Jackson, Rachel Jewell, Alexander C. Chacon, Edith M. Lord, et al. "Intertumoral Genetic Heterogeneity Generates Distinct Tumor Microenvironments in a Novel Murine Synchronous Melanoma Model." *Cancers* 13, no. 10 (May 11, 2021): 2293. https://doi.org/10.3390/cancers13102293.

Rebecca, Vito W., Rajasekharan Somasundaram, and Meenhard Herlyn. "Pre-Clinical Modeling of Cutaneous Melanoma." *Nature Communications* 11, no. 1 (December 2020): 2858. https://doi.org/10.1038/s41467-020-15546-9.

Renkema, Kristin R., Matthew A. Huggins, Henrique Borges da Silva, Todd P. Knutson, Christy M. Henzler, and Sara E. Hamilton. "KLRG1+ Memory CD8 T Cells Combine Properties of Short-Lived Effectors and Long-Lived Memory." *The Journal of Immunology* 205, no. 4 (August 15, 2020): 1059–69. https://doi.org/10.4049/jimmunol.1901512.

Riella, Leonardo V., Alison M. Paterson, Arlene H. Sharpe, and Anil Chandraker. "Role of the PD-1 Pathway in the Immune Response." American Journal of Transplantation: *Official Journal of the American Society of Transplantation and the American Society of Transplant Surgeons* 12, no. 10 (October 2012): 2575–87. https://doi.org/10.1111/j.1600-6143.2012.04224.x.

Robert, Caroline, Antoni Ribas, Jedd D Wolchok, F Stephen Hodi, Omid Hamid, Richard Kefford, Jeffrey S Weber, et al. "Anti-Programmed-Death-Receptor-1 Treatment with Pembrolizumab in Ipilimumab-Refractory Advanced Melanoma: A Randomised Dose-Comparison Cohort of a Phase 1 Trial." *The Lancet* 384, no. 9948 (September 20, 2014): 1109–17. https://doi.org/10.1016/S0140-6736(14)60958-2.

Rosshart, Stephan P., Brian G. Vassallo, Davide Angeletti, Diane S. Hutchinson, Andrew P. Morgan, Kazuyo Takeda, Heather D. Hickman, et al. "Wild Mouse Gut Microbiota Promotes Host Fitness and Improves Disease Resistance." *Cell* 171, no. 5 (November 2017): 1015-1028.e13. https://doi.org/10.1016/j.cell.2017.09.016.

Rudd, Brian D. "Neonatal T Cells: A Reinterpretation." *Annual Review of Immunology* 38, no. 1 (2020): 229–47. https://doi.org/10.1146/annurev-immunol-091319-083608.

Rudd, Christopher E., Alison Taylor, and Helga Schneider. "CD28 and CTLA-4 Coreceptor Expression and Signal Transduction." *Immunological Reviews* 229, no. 1 (May 2009): 12–26. https://doi.org/10.1111/j.1600-065X.2009.00770.x.

Seidel, Judith A., Atsushi Otsuka, and Kenji Kabashima. "Anti-PD-1 and Anti-CTLA-4 Therapies in Cancer: Mechanisms of Action, Efficacy, and Limitations." *Frontiers in Oncology* 8 (March 28, 2018): 86. https://doi.org/10.3389/fonc.2018.00086.

Sun, Xiaoming, and Paul D. Kaufman. "Ki-67: More than a Proliferation Marker." *Chromosoma* 127, no. 2 (June 2018): 175–86. https://doi.org/10.1007/s00412-018-0659-8.

Thomas, Matthew L., and Leo Lefrançois. "Differential Expression of the Leucocyte-Common Antigen Family." *Immunology Today* 9, no. 10 (January 1988): 320–26. https://doi.org/10.1016/0167-5699(88)91326-6.

Wherry, E. John, and Makoto Kurachi. "Molecular and Cellular Insights into T Cell Exhaustion." *Nature Reviews. Immunology* 15, no. 8 (August 2015): 486–99. https://doi.org/10.1038/nri3862.

Wolchok, Jedd D., Vanna Chiarion-Sileni, Rene Gonzalez, Piotr Rutkowski, Jean-Jacques Grob, C. Lance Cowey, Christopher D. Lao, et al. "Overall Survival with Combined Nivolumab and Ipilimumab in Advanced Melanoma." *New England Journal of Medicine* 377, no. 14 (October 5, 2017): 1345–56. https://doi.org/10.1056/NEJMoa1709684.

Xu-Monette, Zijun Y., Mingzhi Zhang, Jianyong Li, and Ken H. Young. "PD-1/PD-L1 Blockade: Have We Found the Key to Unleash the Antitumor Immune Response?" *Frontiers in Immunology* 8 (December 4, 2017): 1597. https://doi.org/10.3389/fimmu.2017.01597.

Yamazaki, Tomohide, Hisaya Akiba, Hideyuki Iwai, Hironori Matsuda, Mami Aoki, Yuka Tanno, Tahiro Shin, et al. "Expression of Programmed Death 1 Ligands by Murine T Cells and APC." *The Journal of Immunology* 169, no. 10 (November 15, 2002): 5538–45. https://doi.org/10.4049/jimmunol.169.10.5538.

Zhang, Zhigang, and Xu Wang. "The Diverse Function of PD-1/PD-L Pathway Beyond Cancer." *Frontiers in Immunology* 10 (2019): 16.